ARTICLE

https://doi.org/10.1590/2317-4889202020190093

BJGEO
Brazilian Journal of Geology

Mineralogy, petrology, and origin of the Pedra Branca Suite: a tonalitic-trondhjemitic association with high Zr, Ti and Y, Carajás Province, Amazonian Craton

Arthur Santos da Silva[1]*, Gilmara Regina Lima Feio[2], João Paulo Silva Alves[3], Roberto Dall'Agnol[4], José de Arimatéia Costa de Almeida[2], Allan Cardek Brunelli Gomes[3]

Abstract

The Pedra Branca suite (2.75 Ga) is located in the Canãa dos Carajás domain in the southeastern Amazonia Craton. It diverges from typical TTG in mineralogical and geochemical terms, by the presence of hornblende and clinopyroxene and because it has a high content of HFSE (Zr, Y, Ti, and Nb). It belongs to the low-K subalkaline series, which varies from metaluminous to peraluminous, and are mostly calc and ferroan granitoids. Amphibole is calcic and classified as ferroan-edenite, and hastingsite. Plagioclase is mainly oligoclase. The Fe/(Fe + Mg) ratios found in the amphiboles indicate that these granitoids were formed under high to moderate fO_2 conditions. Geobarometric calculations suggest pressures between 9.3 and 71 Kbar for the origin and 4.8-53.4 Kbar for the emplacement. Geothermometric calculations suggest initial crystallization temperatures between 945 and 862°C, and the water content in the magma is estimated to be higher than 4 wt%. The magma source was defined as tholeiitic continental gabbro melted in an extensional setting (Carajás Rift) with geochemical features similar to diabase from Nova Canadá (PA). The Pedra Branca magma was originated by partial melting (~28%), leaving a residue with plagioclase (An40), hornblende, clinopyroxene, and may or may not have magnetite.

KEYWORDS: Petrogenesis; Pedra Branca Suite; Carajás Province; Neoarchean.

INTRODUCTION

Archean cratons are commonly composed of greenstone belts and granitoids, among which tonalite-trondhjemite-granodiorite associations stand out (TTG; Windley 1996). Studies about these rocks are essential to understand the dynamics during Archean on Earth (Condie 1994). TTG are the most abundant rock types of the early Archean, found in many cratonic terrains (Smithies 2000, Martin *et al.* 2005, Moyen 2011). They are intermediate to felsic (most > 65 SiO_2 wt%), with high Na_2O/K_2O ratios (> 1.5), low to moderate large-ion litophile elements (LILE), and no potassium enrichment with increased differentiation (Champion and Smithies 2003). These rock associations are derived from rocks with low K and basaltic composition (garnet eclogite), generated by partial melting of subduction slabs (Condie 2005, Martin *et al.* 2005, Martin 1986, Moyen and Martin 2012, Barker and Arth 1976, Barker 1979).

Typical Archean TTG have well-defined and consecrated petrogenetic models geochemical characteristics (Martin 1994). In the Carajás Province (CP), TTG suites have been extensively studied and characterized (Leite *et al.* 2004, Guimarães *et al.* 2010, Almeida *et al.* 2011, 2017, Feio *et al.* 2013, Santos *et al.* 2013b, Silva *et al.* 2014). The Pedra Branca Suite (PBS; Gomes and Dall'agnol 2007, Feio *et al.* 2013) outcrops in Canaã dos Carajás region, southeastern Pará State, Brazil. This tonalite-trondhjemite suite shows both similarities and differences with typical Archean TTG. It is similar to TTG suites in classificatory terms such as low Sr, K content and low K/Na ratios, however, diverge from TTG since it has distinct geochemical features such as high HFSE content (Ti, Zr, Y, and Nb), low transitional elements (Cr and Ni). Another characteristic comparing to other TTG rocks from Rio Maria Domains in the CP is the presence of amphibole and relicts of clinopyroxene (Sardinha *et al.* 2004, Gomes and Dall'agnol 2007, Feio *et al.* 2013, Sousa 2015).

---

[1] Universidade de Brasília – Brasília (DF), Brazil. E-mail: santos_arthur@hotmail.com

[2] Universidade Federal do Sul e Sudeste do Pará – Marabá (PA), Brazil. E-mail: gilmarafeio@unifesspa.edu.br, ari@unifesspa.edu.br

[3] Universidade Federal do Pará – Belém (PA), Brazil. E-mails: joao.p-17@hotmail.com, alanbrunelli@gmail.com

[4] Instituto Tecnológico Vale – Belém (PA), Brazil. E-mails: robdal@ufpa.br

*Corresponding author.

Supplementary data

Supplementary data associated with this article can be found in the online version: Supplementary Table A1, Supplementary Table A2, Supplementary Table A3, Supplementary Table A4, Supplementary Table A5, Supplementary Table A6, Supplementary Table A7, Supplementary Table A8.

In this sense, this paper had integrated field data; petrography, mineral chemistry, geochemistry, and geochemical modeling to elaborate a petrogenetic model to Pedra Branca Suite and, thus, unravel the role of these rocks in the evolution of Canaã dos Carajás Domain.

GEOLOGICAL SETTING

The Carajás Province (Fig. 1) is located in the southeastern portion of the Amazonian Craton, in the geologic context of the Amazonia Central Province (Tassinari and Macambira 2004) or the Carajás Province (Santos *et al.* 2006). The CP represents the oldest portion of the Amazonian Craton (Tassinari and Macambira 2004, Santos *et al.* 2006). The Carajás Province is divided into four tectonic domains according to Dall'Agnol *et al.* (2013): Rio Maria Domain (RMD), Sapucaia Domain (SD), Canaã dos Carajás Domain (CCD), and Carajás Basin (CB).

The Rio Maria Domain was formed between 3.0 and 2.86 Ga (Machado *et al.* 1991, Macambira and Lafon 1995, Almeida *et al.* 2011). The domain is composed of greenstone belts, TTG assemblages, leucogranodiorites, high-Mg granitoids, and potassic granites (Althoff *et al.* 2000, Souza *et al.* 2001, Dall'Agnol *et al.* 2006, Oliveira *et al.* 2010a, Almeida *et al.* 2011, 2013).

The main units of the Sapucaia domain (2.95–2.73 Ga; Oliveira *et al.* 2010b, Dall'Agnol *et al.* 2013, Gabriel and Oliveira 2014, Santos *et al.* 2013b, Silva *et al.* 2014, Santos and Oliveira 2014, Rodrigues *et al.* 2014) are similar in lithologic

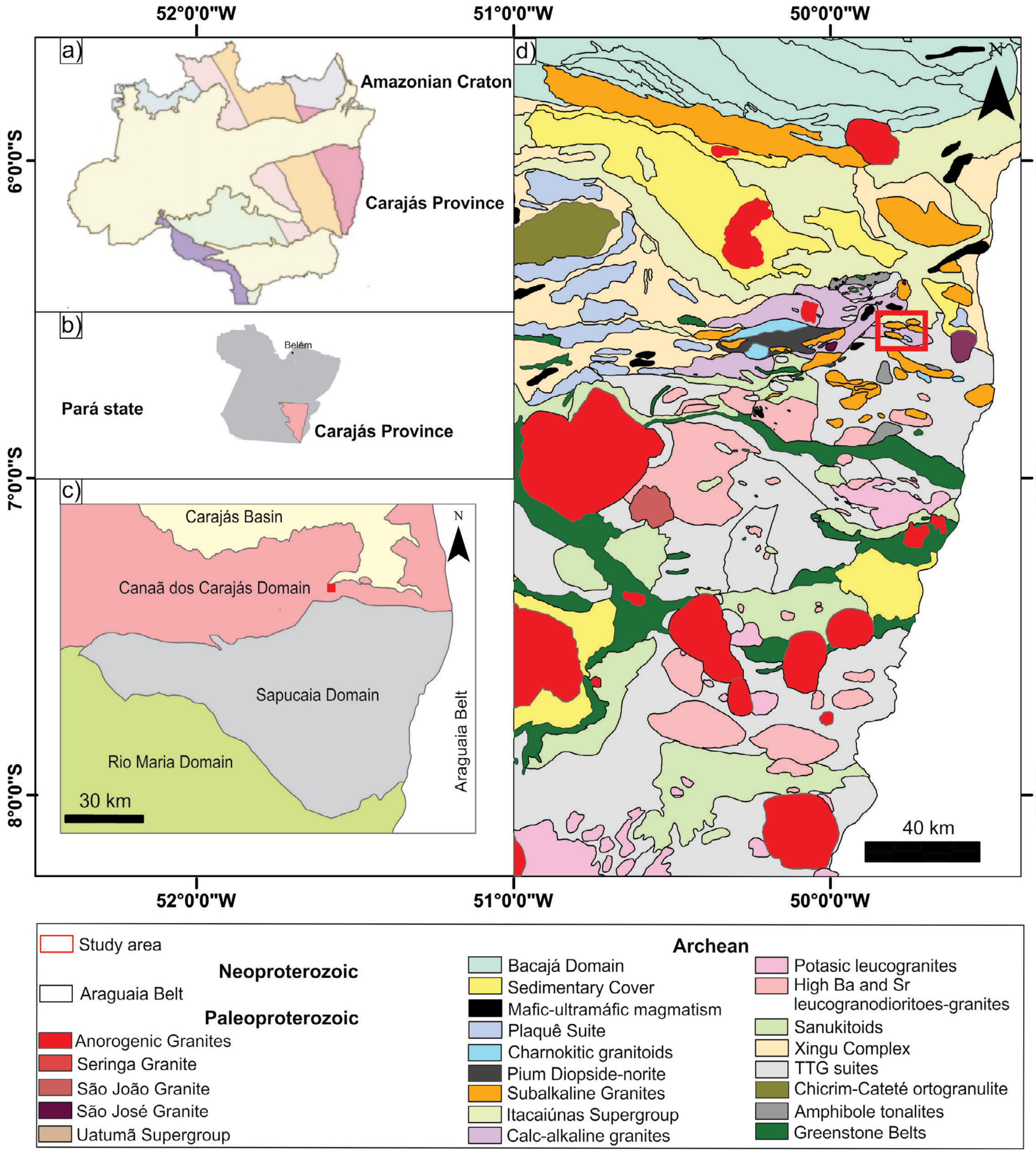

Figure 1. (A) Amazonian Craton provinces map (Santos *et al.* 2006); (B) Pará state map highlighting Carajás Province; (C) simplified map showing the Carajás Province compartmentation; (D) lithological map from Carajás Province. Altered from Teixeira (2017) and references therein.

terms to the dominant rocks in the Rio Maria domain, but the former was strongly affected by Neoarchean tectonic events and intruded by plutons of the Vila Jussara Suite.

The Canaã dos Carajás domain differs from SD and RMD in terms of lithologic associations, deformation and Nd isotopic signatures (Dall'agnol *et al.* 2013, Feio *et al.* 2013). Previous studies performed at the CCD indicate that this domain underwent a more complex evolution and various magmatic events have been distinguished (Feio *et al.* 2013):

- at ~3 Ga, the formation of the Bacaba Tonalite (Moreto *et al.* 2011);
- at 2.96–2.93 Ga, emplacement of the Canaã dos Carajás Granite and the Rio Verde Trondhjemite;
- at 2.87–2.83 Ga, crystallization of the Campina Verde Tonalitic Complex, Rio Verde Trondhjemite and Cruzadão, Bom Jesus and Serra Dourada granites;
- finally, during the Neoarchean, at 2.75–2.72 Ga, the Planalto Suite, the Pedra Branca Suite, and the charnockitic assemblages (Pium Complex) were formed (Feio *et al.* 2012, 2013; Santos *et al.* 2013a).

The main assemblages of the Carajás Basin are of Neoarchean age (~2.76 Ga; Gibbs *et al.* 1986, Machado *et al.* 1991). They are composed predominantly of mafic to intermediate metavolcanic rocks and banded iron formations, both included in the Itacaiúnas Supergroup. The latter is intruded by the Neoarchean (~2.75–2.73 Ga) Estrela, Igarapé Gelado, and Serra do Rabo granites.

RESULTS

Field Aspects and Petrography

Previous geological mapping performed in the Canaã dos Carajás region (Feio *et al.* 2013, Gomes 2003, Gomes and Dall'Agnol 2007, Sardinha *et al.* 2004) were able to recognize and individualize several geologic units previously encompassed in the Xingu Complex, among which the Pedra Branca suite.

The rocks from PBS occupy a restricted area and are represented by two bodies (Fig. 2). This suite is formed by tonalites and trondhjemites. In the "south body", the rocks are very deformed, showing magmatic banding striking near E-W with alternation between tonalitic and trondhjemitic bands and sub-vertical foliation striking E-W. In the "north body", rocks are mainly isotropic, showing tonalitic and trondhjemitic domains. The PBS is admittedly intrusive in the Planalto suite and Itacaiunas Supergroup, although field relations are not entirely conclusive (Gomes and Dall'Agnol 2007).

The petrographic studies were performed on 13 thin sections at the petrography laboratory of the Instituto de Geociências e Engenharias from Universidade do Sul e Sudeste do Pará (Unifesspa). The mineral abbreviation followed the rules suggested by Whitney and Evans (2010). The rocks from PBS are tonalites and trondhjemites (Fig. 3) and have a fine-grained, equigranular allotriomorphic texture (Figs. 4A and 4D) with variation to medium-grained. They show intense deformational textures such as mylonitic texture and polygonal grain-boundary (Figs. 4B and 4E). Tonalites are mesocratic and trondhjemites hololeucocratic

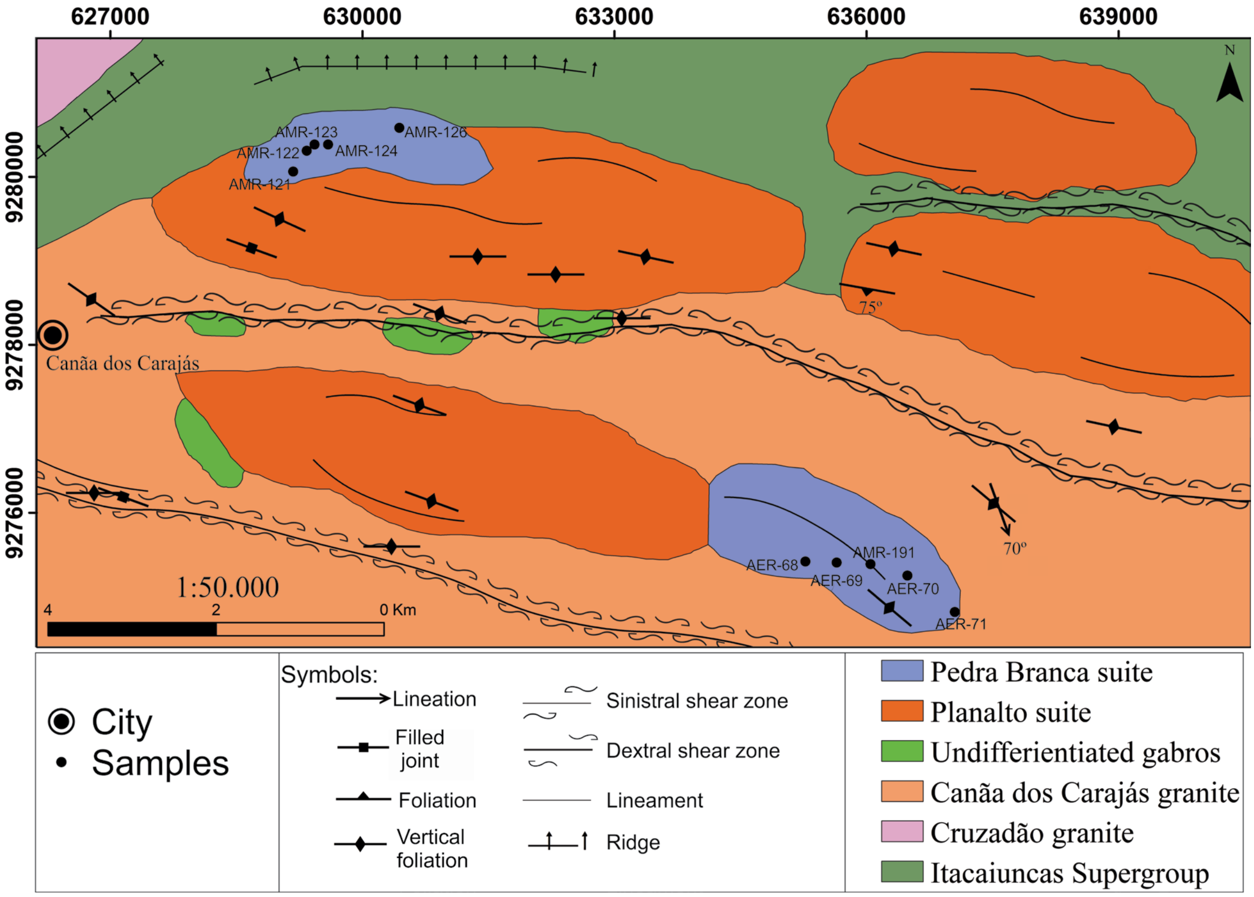

Source: Feio *et al.* (2013).

Figure 2. Geologic map showing the occurrence of the tonalites and trondhjemites from Pedra Branca suite, Canaã dos Carajás county

(Fig. 4C). The main mineralogy in tonalites and trondhjemites is represented by plagioclase (An_{16}-An_{23}) and quartz, alkali-feldspar crystals are rare. Hornblende is the main mafic mineral in tonalites, and biotite in trondhjemites. In some places clinopyroxene remnants can occur in tonalites. Accessory minerals in tonalites and trondhjemites include titanite (Fig. 4F), zircon, apatite, and muscovite; secondary minerals are tourmaline, scapolite, epidote, and sericite (Gomes and Dall'agnol 2007). Opaque minerals in both tonalites and trondhjemites are ilmenite (Fig. 4F) and magnetite.

Geochemistry

The chemical analyses for major and trace elements, including rare earth elements (REE), was performed by Inductively Coupled Plasma Emission Spectrometer (ICP-ES) and Inductively Coupled Plasma Mass Spectrometry (ICP-MS), respectively, at the Acme Analytical Laboratories Ltda. in Canada. The representative chemical compositions of the Pedra Branca Suite are given in Table 1 and illustrated in Harker diagrams (Figs. 5 and 6).

Silica contents range from 55.74 to 79.52 wt%; these rocks show high TiO_2 content and low Al_2O_3. They can be classified as low aluminium (Al) TTG (15% ≥), except for sample AER-70 (Barker and Arth 1976). The rocks from the Pedra Branca suite show negative correlation trends of silica with the major oxides TiO_2, Al_2O_3, FeO, MnO, MgO, CaO, and P_2O_5; they also show a slight increase in K_2O with silica content, and there is no clear correlation between silica and Na_2O. The rocks from this suite are impoverished in K_2O (0.49–0.93 wt%); they show low K_2O/Na_2O ratios (0.09–0.19).

In terms of trace elements, this Suite shows low content of Ba, Rb, and Sr. Tonalites varieties in PBS displays greater values of Sr and #Mg if compared to trondhjemites. All samples are enriched in high field-strength elements (HFSE) [Zr (168–667.10 ppm), Y (1.60–50.30 ppm)] and relatively enriched in Nb (2.90–25.00 ppm). Rb display a positive correlation with silica content; on the order hand, Sr, Y, Ni, V, and #Mg show a negative correlation with silica. There is no clear correlation between Cr and silica; all rocks have similar Cr values.

Normalized REE patterns are given in Figure 7. The PBS is enriched in light rare earth elements (LREE) and slightly depleted in heavy rare earth elements (HREE). Tonalites are more enriched in REE than trondhjemites, they show discrete Eu anomalies (positive and negative), except for sample AMR-121C; on the order hand, trondhjemites show high positive Eu anomalies. All samples have low (La/Yb)n ratios (0.73–1.33).

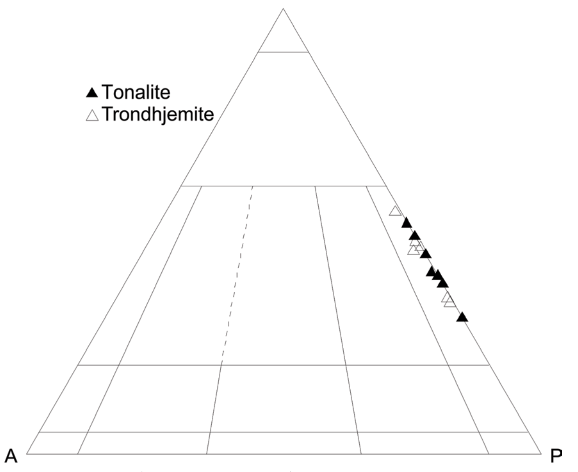

Figure 3. QAP (Le Maitre 2002) classification of the granitoids from PBS (Gomes and Dall'Agnol 2007).

The classifications based on major elements are given in Fig. 8. PBS rocks vary from tonalites to trondhjemites according to Ab-An-Or (Fig. 8A, O'Connor 1965); on SiO_2 *vs.* K_2O diagram (Fig. 8C, fields of Le Maitre *et al.* 2002) all samples plot in the low-K field. Tonalites are metaluminous, and trondhjemites vary between metaluminous and peraluminous (Fig. 8D, Shand 1943). In Frost *et al.* (2001), diagrams FeOt/(FeOt + MgO) *vs.* SiO_2 and $K_2O + Na_2O$-CaO *vs.* SiO_2 plot mostly in calcic (Fig. 8E) and ferroan (Fig. 8F) fields, respectively. They have moderate to high ferromagnesian, with FeOt+MgO values ranging between 4.41 and 14.48 wt%.

Mineralogy

Representative samples of the Pedra Branca suite were selected for mineral chemical analyses. The analyzed minerals were amphibole, plagioclase, titanite, and iron-titanium oxides. Polished thin sections of the selected samples were initially submitted to semiquantitative chemical analysis by energy dispersive spectroscopy (EDS) in the LEO 1430 SEM of the Laboratório de Microanálises da Universidade Federal do Pará, which were performed at an accelerating voltage of 20 kV. The samples were also submitted to wavelength dispersive spectroscopy (WDS) quantitative analyses at the Laboratório de Microssonda da Universidade de Brasília, using a JEOL JXA-8230 electron probe microanalyzer (EPMA), which were performed under the following operating conditions: column accelerating voltage of 15 kV; current of 10 nA; analysis time of 10 s for peak and background radiation. The matrix effects were correct within the EPMA software by the ZAF method. The standards used for instrument calibration were andradite (Ca and Fe), microcline (Si, Al, and K), olivine (Mg), albite (Na), pyrophanite (Ti and Mn), vanadinite (V and Cl), nickel oxide (Ni), chromium trioxide (Cr), and Celestine (Sr). All thin sections selected for electron microprobe analyses were previously carbon-coated.

Amphibole

Amphibole analyses (Suppl. Tabs. 1 and 2) were performed using free-H_2O content, and the structural formula was calculated based on 23 oxygen atoms, according to the method of Leake *et al.* (1997). For structural formula calculation, the cations were collected into a set of 13 cations minus Ca, Na, and K. Amphiboles were classified (Fig. 9) according to the criteria of Leake *et al.* (1997).

The Pedra Branca suite has a calcium amphibole classified as hastingsite and ferroan-edenite [$(Ca + Na)B \geq 1.00$ and $NaB < 0.50$] according to Leake *et al.* (1997). Still according to these authors, the amphiboles from PBS fit in the first parameter [$CaB \geq 1.50$; $(Na + K)A \geq 0.50$]. The Si content in the amphiboles vary between 6.14 and 6.59. Mg/(Mg + Fe) ratio varies between 0.38 and 0.49. Fe/(Fe + Mg) ratio between 0.51 and 0.59. Al_{total} between 1.63 and 2.50.

Epidote

Representative chemical analyses of epidote from the Pedra Branca suite are presented in Supplementary Table 3.

The criteria indicated by Tulloch (1979) was used to evaluate the magmatic *vs.* subsolidus origin of the studied epidote crystals, based on the 'pistacite' component (Ps = molar [Fe^{3+}/Fe^{3+} + Al] / 100).

The 'pistacite' component varies between 17 and 23 (Fig. 10), considered by Tulloch (1979) as typical of subsolidus alteration of plagioclase.

Plagioclase

Representative chemical analyses of plagioclase from the Pedra Branca suite are presented in Supplementary Table 4. The plagioclase shows an average composition of An_{18} (An_{20} - An_{16}) classifying oligoclase.

Titanite

Titanite has no significant compositional difference (Suppl. Tabs. 5 and 6). It shows a Fe/Al ratio varying between 0.43 and 0.84. Titanite plot mostly near the field of metamorphic titanite and subordinately near the igneous titanite (Fig. 11). Therefore, the titanite was initially formed in a magmatic state and posteriorly underwent a compositional rebalance due to a deformational or a superimposed metamorphic event.

Iron-titanium oxide minerals

Preliminary chemical compositions were obtained by EDS (Suppl. Tab. 7). Ilmenite is the main iron-titanium oxide.

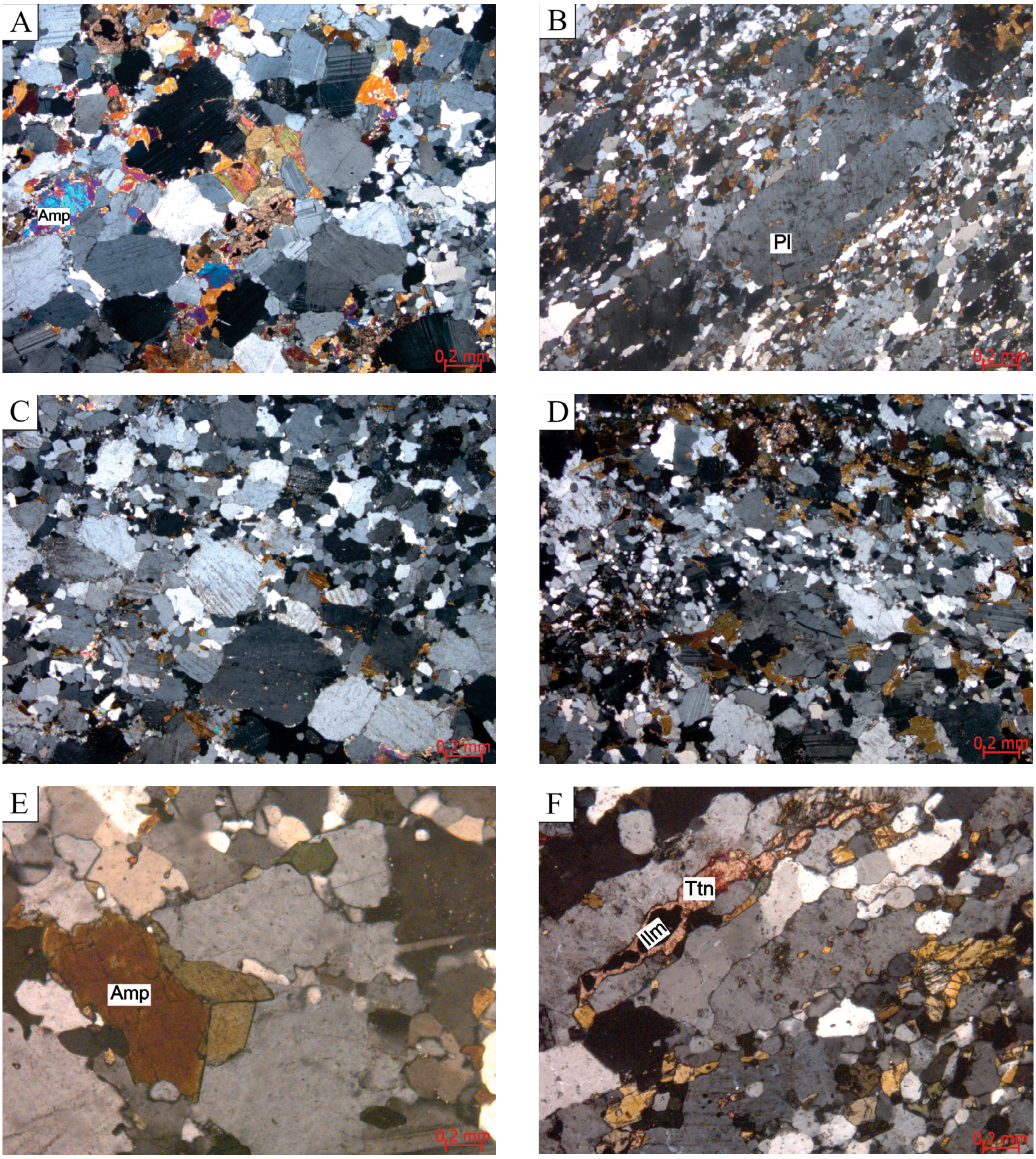

Figure 4. Petrographic aspects of the tonalites and trondhjemites from PBS: (A) granular allotriomorphic texture in tonalite (AMR-124A); (B) Mmlonitic tonalite (AER-68); (C) granular hypidiomorphic serial texture in trondhjemite (AMR-124B); (D) granular hypidiomorphic serial texture in tonalite (AMR-121E); (E) polygonal contact between amphibole crystals (Amp) (AMR-123); ilmenite crystals (Ilm) with titanite (ttn) corona (AER-71C).

It was deduced that ilmenite crystals are primary and originated during Pedra Branca crystallization, based on petrographic observations. The magnetite was re-equilibrated during the suite evolution, and its composition is similar to that of pure magnetite.

Geochemical modeling

Major and trace element modeling was performed to assess the origin of the Pedra Branca suite, using the Genesis 4.0 software (Teixeira 2005). The mineral/liquid partition coefficients (KD) used in the modeling are given in the Supplementary

Table 1. Chemical composition of the granitoids of the Pedra Branca Suite in wt%

Samples	Tonalite							Trondhjemite					
	AMR-124A	**AMR-122C**	**AMR-121D**	**AMR-123**	**AMR-121A**	**AER-68**	**AER-71C**	**AER-70**	**AMR-124B**	**AMR-121E**	**AMR-191A**	**AER-69B**	**AMR-126A**
SiO_2	55.74	62.67	64.03	65.36	66.50	71.38	72.68	73.70	74.85	75.42	77.26	77.60	79.52
TiO_2	1.77	1.28	1.39	1.27	1.32	0.84	0.34	0.55	0.51	0.46	0.34	0.59	0.19
Al_2O_3	13.25	14.07	14.29	14.21	14.98	13.62	13.21	15.14	14.11	14.03	13.25	12.61	11.42
FeO	10.42	7.83	5.33	5.70	2.83	2.75	2.38	0.22	1.16	0.92	0.25	0.39	1.12
Fe_2O_3	11.58	8.70	5.92	6.34	3.14	3.06	2.65	0.25	1.29	1.02	0.28	0.43	1.24
MnO	0.13	0.06	0.07	0.07	0.07	0.02	0.02	< 0.01	0.02	0.01	< 0.01	< 0.01	< 0.01
MgO	4.16	1.30	1.58	1.46	1.87	0.55	0.91	0.02	0.03	0.03	0.01	0.05	0.11
CaO	8.01	4.88	6.22	4.84	5.95	3.83	3.57	2.47	2.03	2.26	2.39	2.21	0.93
Na_2O	3.81	5.12	4.92	4.97	4.91	5.19	4.73	6.14	5.28	5.24	5.19	5.17	4.81
K_2O	0.62	0.68	0.53	0.63	0.50	0.62	0.55	0.62	0.75	0.71	0.57	0.57	0.93
P_2O_5	0.43	0.30	0.40	0.06	< 0.01	0.15	0.07	< 0.01	< 0.01	< 0.01	< 0.01	< 0.01	0.01
LOI	0.30	0.80	0.50	0.60	0.60	0.60	1.10	0.90	1.00	0.70	0.60	0.60	0.70
Ba	198.00	207.00	193.00	310.00	204.00	137.00	65.00	157.00	277.00	234.00	102.00	157.00	303.00
Rb	8.60	12.10	6.20	8.20	13.90	12.10	20.70	15.80	19.30	17.50	10.80	13.60	29.90
Sr	241.30	279.40	299.00	288.30	316.00	207.30	184.70	219.60	230.40	237.30	193.00	185.00	132.10
Zr	168.10	415.00	335.80	476.30	416.50	667.10	388.80	528.70	299.50	245.80	429.70	602.60	239.20
Nb	6.80	20.70	25.00	24.60	21.10	11.80	7.30	10.30	4.60	2.90	8.20	8.80	10.20
Y	16.40	30.00	34.60	29.10	13.10	50.30	30.20	12.40	1.60	1.30	11.10	7.70	3.70
Th	4.30	18.10	15.10	19.70	25.60	8.00	20.20	1.70	21.10	32.10	8.80	5.10	16.00
Ni	7.70	< 20	3.60	< 20	< 20	5.10	9.90	2.20	< 20	1.00	< 20	< 20	1.60
Co	40.10	32.70	33.50	30.50	36.40	8.80	108.20	94.30	28.40	43.60	1.30	70.50	57.90
Zn	8.00	9.00	7.00	5.00	5.00	5.00	10.00	6.00	4.00	4.00	4.00	7.00	4.00
La	11.00	8.30	9.60	4.80	5.00	15.40	5.90	14.40	2.00	1.90	7.90	12.10	6.00
Ce	34.40	20.20	24.50	8.60	5.90	33.90	10.80	13.30	3.00	2.70	16.80	12.00	10.50
Pr	5.35	3.40	3.61	2.02	1.42	6.21	1.72	3.24	0.26	0.24	2.45	2.71	1.16
Nd	24.90	17.50	17.30	9.60	5.60	33.60	8.50	12.70	1.00	0.90	10.10	9.60	4.50
Sm	4.55	4.52	4.14	3.05	1.47	8.06	2.64	2.13	0.16	0.13	1.69	1.57	0.84
Eu	1.57	1.11	1.21	1.67	1.37	2.34	0.88	1.14	0.90	0.83	0.98	1.16	1.04
Gd	3.72	4.76	4.72	4.00	1.53	8.92	3.78	2.06	0.08	0.13	1.53	1.38	0.78
Tb	0.54	0.77	0.65	0.83	0.30	1.41	0.72	0.32	0.02	0.02	0.27	0.24	0.10
Dy	3.07	4.34	4.26	5.38	2.17	8.25	4.52	1.93	0.19	0.15	1.59	1.43	0.59
Ho	0.60	0.91	0.92	1.19	0.43	1.67	1.02	0.39	0.05	0.04	0.33	0.30	0.13
Er	1.78	2.63	2.69	3.86	1.47	4.95	3.32	1.17	0.20	0.18	1.12	0.91	0.37
Tm	0.25	0.41	0.42	0.66	0.25	0.70	0.59	0.18	0.05	0.03	0.19	0.16	0.05
Yb	1.85	2.71	2.84	4.69	1.92	4.40	3.87	1.39	0.41	0.35	1.28	1.10	0.38
Lu	0.31	0.44	0.47	0.75	0.32	0.70	0.69	0.25	0.08	0.06	0.21	0.18	0.07
V	306.00	104.00	65.00	57.00	39.00	41.00	35.00	< 8	< 8	< 8	8.00	< 8	13.00
Cr	-	99.85	-	99.83	99.84	-	-	-	99.89	-	99.90	99.86	-
K_2O/Na_2O	0.16	0.13	0.11	0.13	0.10	0.12	0.12	0.10	0.14	0.14	0.11	0.11	0.19
*Mg	0.42	0.23	0.35	0.31	0.54	0.26	0.40	0.14	0.04	0.06	0.07	0.19	0.15
FeO/(FeO+MgO)	0.71	0.86	0.77	0.80	0.60	0.83	0.72	0.92	0.97	0.97	0.96	0.89	0.15
Eu/Eu*	1.13	0.73	0.83	1.46	2.77	0.84	0.85	1.64	21.63	19.31	1.83	2.35	3.86

Table 8; most of them are from the software (Genesis 4.0) and Rollison (1993) and references therein.

Geochemical modeling was focused on hornblende tonalite (AMR-124A). This rock was interpreted to represent the parental magma because it has the lowest silica and highest ferromagnesian contents. Two hypotheses were considered to explain the origin of the Pedra Branca magma:

- partial melting of a mafic source;
- contamination of a mafic magma by the less evolved facies from Planalto A-type granite (Feio *et al.* 2012).

Therefore, some possible magma sources were selected:

- High Ti Basalt from Paraná (Wilson 1989);
- Archean Basalts (Condie 1993);
- Diopside-Norite Pium (Feio *et al.* 2013, Santos *et al.* 2013a);
- Diabase from Nova Canadá-PA (Marangoanha and Oliveira 2014).

Furthermore, geochemical data from mafic rocks (Condie 1993, Kepezhinskas *et al.* 1995, Santos *et al.* 2013a, Souza *et al.* 2001, Takahashi 1986) were contaminated from 2 to 30% using simple mixture models provided by the Genesis 4.0 software (Teixeira 2005), by the least evolved facies from Planalto Granite (Feio *et al.* 2012). Source 4 (Hornblende Gabbronorite, ADK-43, Marangoanha and Oliveira 2014) exhibited satisfactory results to major elements modeling (partial melting or crystal fractionation). The other sources exhibited unsatisfactory results.

Moreover, modeling using the least evolved (AMR-124A) and the most evolved (AMR-126A) samples from this suite were performed using mineral chemistry data, showing unsatisfactory results. Therefore, the modeling discussed throughout this work is valid to explain only the origin of tonalites from PBS.

For major elements, six models were obtained with distinct mineralogical residual assemblage; in two models, results for major and trace elements were satisfactory. In the first model,

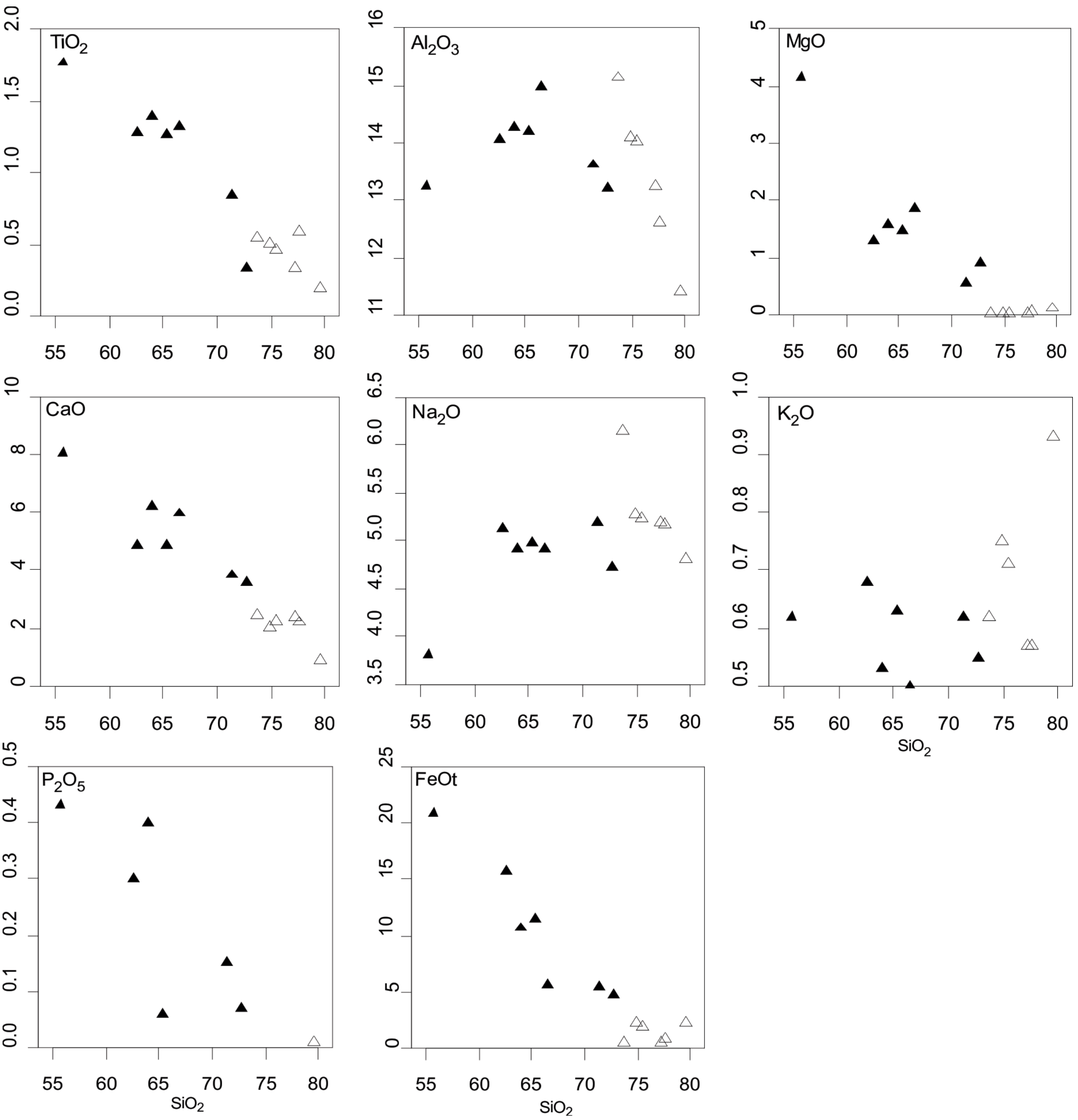

Figure 5. Harker diagrams (Silica *vs.* major elements). Symbology according to Figure 3.

the residual assemblage was composed of clinopyroxene, hornblende, and plagioclase (An_{40}). The second model was composed of clinopyroxene, hornblende, plagioclase (An_{40}), and magnetite. The results of both modelings are exposed in Table 2 (Fig. 12).

DISCUSSION

Geochemistry as petrogenetic indicator

The rocks from PBS belong to the Low-Al TTG group (Barker and Arth 1976), they have a lower content of Sr and Eu, less fractionated REE, and low Sr/Y ratios compared to High-Al TTG. Moreover, these suits show low values of $(La/Yb)_N$. These characteristics imply a petrogenesis outside the garnet stability field and were controlled by plagioclase, either by being a main residual phase or by its fractionation during magmatic differentiation (Almeida *et al.* 2011, Moyen and Stevens 2006).

The mineralogical assemblage of the liquid that generated the PBS reflects directly in the geochemical features of the rocks. As exposed in the Harker diagrams (Fig. 5), CaO, MnO, MgO, TiO_2, and Y show a negative relation with the silica content, as opposed to K_2O, Rb, and Ba, which show a positive one. These trends tend to

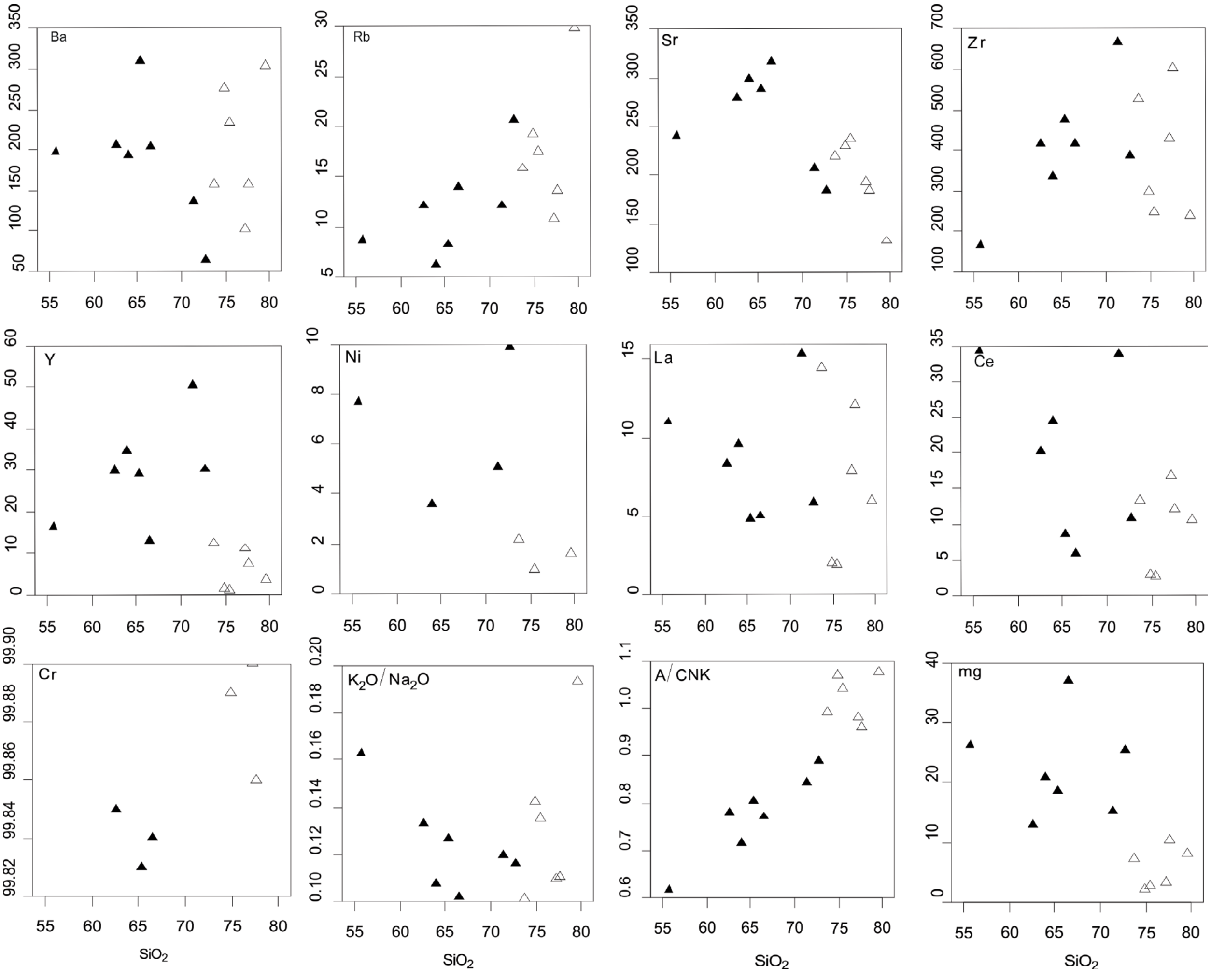

Figure 6. Harker diagrams (Silica *vs.* trace elements). Symbology according to Figure 3.

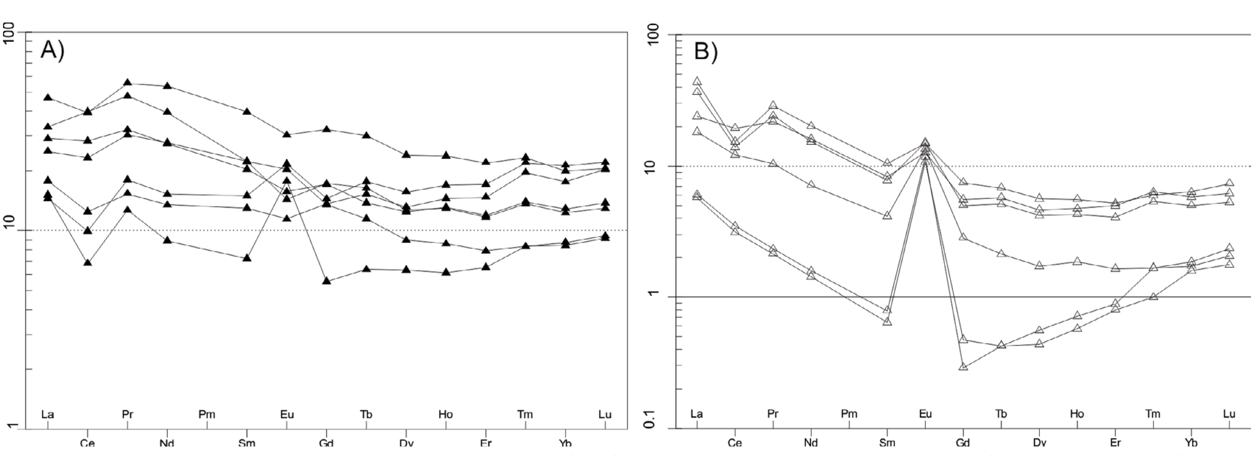

Figure 7. Chondrite normalized REE patterns (Nakamura 1974); (A) tonalites showing discrete Eu anomalies (positive and negative) except in one sample; (B) trondhjemites showing high positive Eu anomalies. Symbology according to Figure 3.

occur when the fractionation is dominated by ferromagnesian phases such as amphibole and calcic plagioclase (Janoušek *et al.* 2000).

Tonalite REE enrichment compared to trondhjemites implies the fractionation of mineral phases with higher KD, like amphibole, or due to amphibole accumulation during magmatic flow (Suppl. Tab. 8; Janoušek *et al.* 2000).

Parental magma

The most primitive rock from the PBS is the hornblende tonalite (AMR-124A) with 55.74 wt% SiO_2. This rock has the highest compatible element content (*i.e.,* Ca, Mg, Fe, Ti, P, and V) and the lowest incompatible element content (*i.e.,* K, Th, and U). Therefore, the AMR-124A is assumed to represent

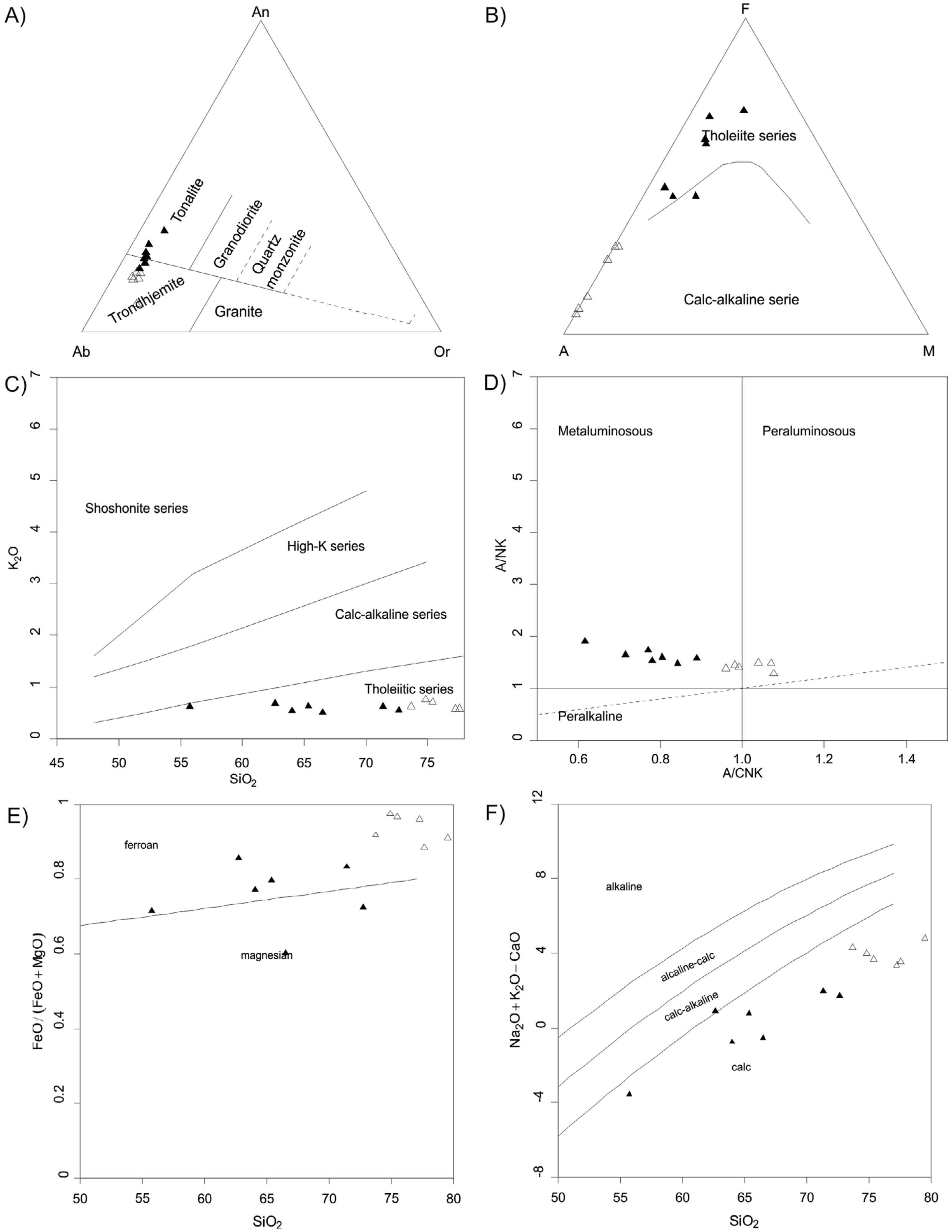

Figure 8. (A) Ab-An-Or diagram; (B) AFM diagram; (C) SiO2 *vs.* K2O diagram; (D) A/NK *vs.* A/CNK diagram; (E) FeOt/(FeOt + MgO) *vs.* SiO2 diagram; (F) Na2O + K2O-CaO *vs.* SiO2 diagram. Symbology according to Figure 3.

the parental magma of PBS, whose composition is much less siliceous than the average Archean low-Al TTG suite (~71 wt% SiO2, Almeida *et al.* 2011, Zhang *et al.* 2012). The REE pattern of the assumed parental magma of the Pedra Branca suite can be reproduced using a tholeiitic source with flat REE pattern (ADK43, Marangoanha and Oliveira 2014), moderate degrees of partial melting (~ 28%) and a residue with 21.39% Cpx + 70.74 % Hbl + 7.86 % Pl (An40) 7.86 % or 16.23% Cpx + 53.59% Hbl +27.35% Pl (An40) + 2.84% Mt.

Magmatic differentiation

Several diagrams were constructed to unravel the processes responsible for differentiation in tonalites from PBS.

Crystallization in plutonic rocks of hornblende, plagioclase, and accessory Fe-Ti oxides, zircon, and apatite are indicated by the negative correlation of silica with Ca, Fe, Mg, and Ti, as well as by trace elements such as V, Sr, and Y (Seixas *et al.* 2012). According to Martin (1987), crystal fractionation and partial melting can be evaluated by plots of the granitoids samples in logarithmic graphs of compatible elements *versus* incompatible elements in the suite, in this case, were elaborated graphs of V (compatible) *versus* Rb and Th (incompatible) (Fig. 13). It is also important to notice that magmas originated by fractionation crystallization or partial melting, assuming identical bulk distribution coefficient, show distinctive trends (Cocherie 1986).

The magmatic differentiation process can also be analyzed by covariant diagrams of K_2O, Sr, Y, and Zr as a function of the CaO content and Mg# (Fig. 14), once that both CaO and Mg# are affected by hornblende and plagioclase and both are

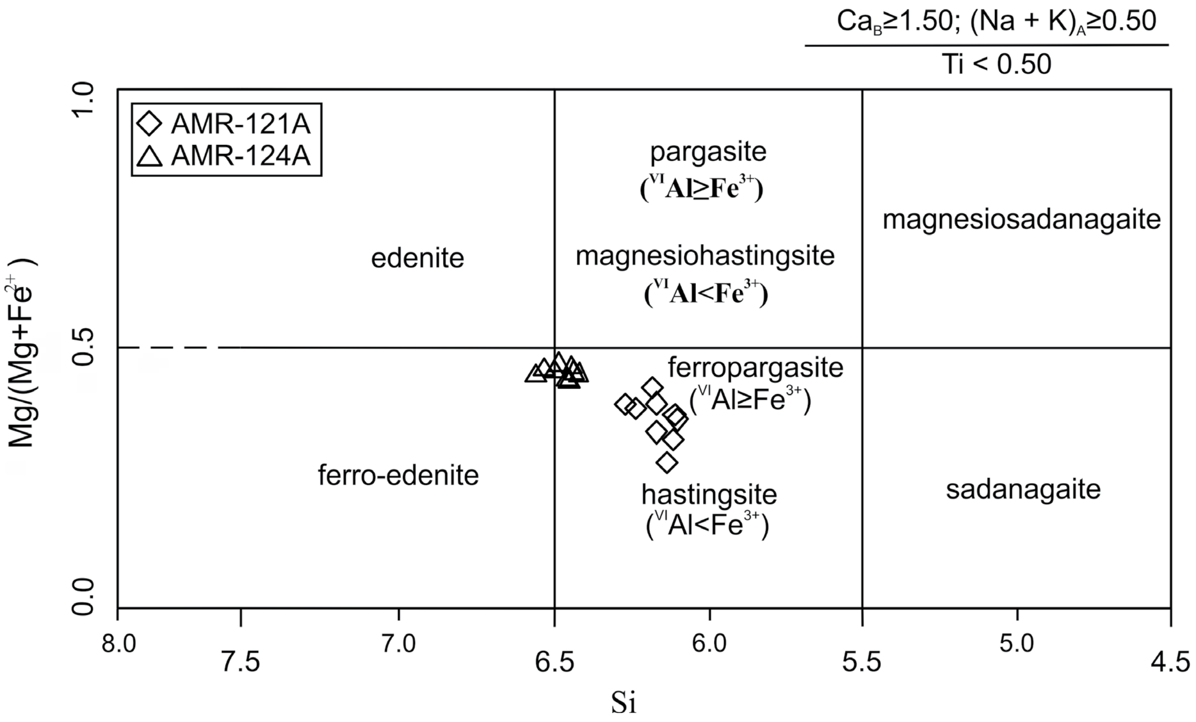

Figure 9. Classification diagram (Leake *et al.* 1997) for the amphibole of the Pedra Branca suite.

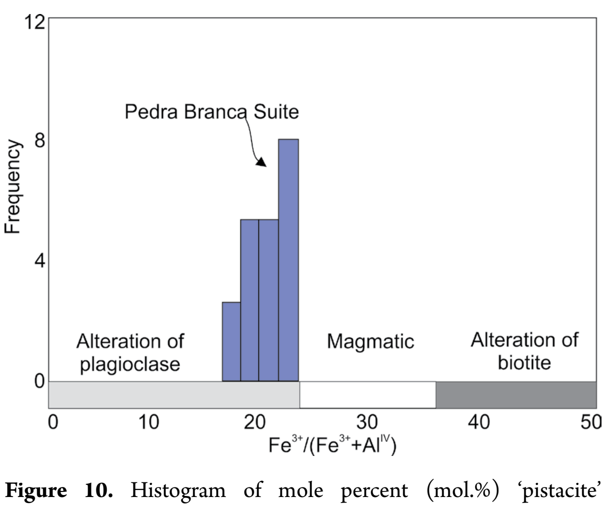

Figure 10. Histogram of mole percent (mol.%) 'pistacite' component (Ps) epidotes from different rocks of the Pedra Branca Suite. The compositional ranges of epidote from the alteration of plagioclase and biotite are from Tulloch (1979).

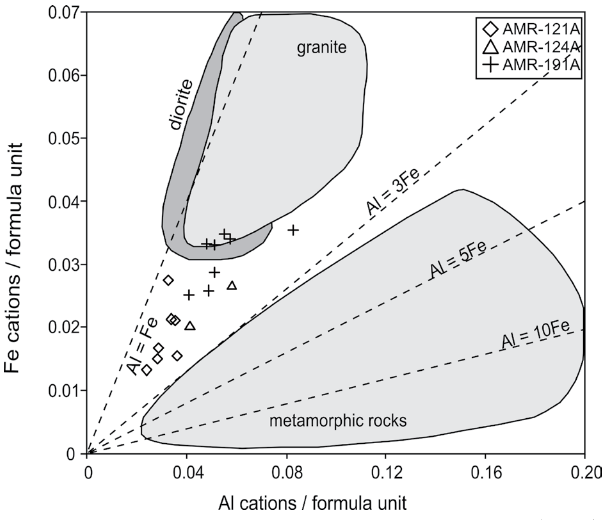

Figure 11. Fe *vs.* Al diagram Aleinikoff *et al.* (2002) compositional fields of magmatic and metamorphic titanite Kowallis *et al.* (1997).

present in PBS tonalites. Geochemical variations against these proxies can be used to examine the influence of amphibole and plagioclase fractionation on tonalitic suites (Arth *et al.* 1978, Kalsbeek 2001).

Therefore, the PBS tonalitic rocks range from 55.74 to 72.68 wt% SiO_2, showing scattered inter-element correlation in the Harker diagrams between the low and high silica members. The other evaluated diagrams (Figs. 13 and 14) also show a scattered pattern and do not reproduce the hypothetical liquid line starting from the proposed parental magma. These features do not suggest that crystal fractionation nor partial melting were the mechanisms to explain the magmatic differentiation of the suite, so we suggest that the main process was the crystal accumulation during the magmatic flow.

Table 2. Geochemical modeling data for the Pedra Branca suite (values in wt%).

Sample	**ADK 43**	**AMR-124A**	**Cs1**	**Cs2**
Lithology	**Horblende Gabbronorite**	**Hornblende Tonalite**		
SiO_2	51.05	56.02	48.69	48.66
TiO_2	0.86	1.78	1.11	0.93
Al_2O_3	13.88	13.32	13.85	13.79
Fe_2O_3	13.49	11.64	13.75	13.88
MnO	0.21	0.13	0.06	0.03
MgO	10.83	8.05	8.67	11.85
CaO	1.98	3.83	11.34	2.19
Na_2O	0.45	0.62	1.99	0.42
K_2O	0	0.43	0.55	0
Ni	28	7.70	6.64	7.66
Rb	15.7	8.60	23.40	19.23
Ba	122	198.00	194.00	188.00
Sr	92.8	241.30	125.00	120.00
Nb	3.4	6.80	4.70	5.06
Zr	68.4	168.10	109.00	104.00
Y	23	16.40	17.06	19.81
La	7.5	11.00	11.48	11.61
Ce	14.3	34.40	21.87	22.24
Nd	7.5	24.90	11.86	11.43
Sm	2.32	4.55	2.66	2.98
Eu	0.79	1.57	0.68	0.74
Gd	3.01	3.72	2.48	2.94
Tb	0.59	0.54	0.45	0.54
Dy	4.11	3.07	3.13	3.75
Er	2.5	1.78	1.98	2.37
Yb	2.39	1.85	2.06	2.44
Lu	0.28	0.31	0.24	0.29
Residue composition (%)				
Plagioclase An 40			7.86%	27.35%
Clinopyroxen			21.39%	16.23%
Hornblende			70.74%	53.59%
Magnetite				2.84%
F			27%	28%
Σr^2			0.944	0.809

Partial melting formula:
$Cl/Co = 1/D\ (1-F)^{(1/D-1)}$ (Wilson 1989)
Cl – liquid composition
Co – original solid composition
D – distribuition coefficient
(1-F) – crystal fraction rate
F- melting rate
r^2 sum of residue

Crystallization parameters

Temperature

Ridolfi *et al.* (2010) and Ridolfi and Rezulli (2012) reviewed thermobarometric equations in the literature and have shown calibration models to estimate temperature using the content of the main oxides in the amphibole. Those equations are recommended to amphiboles crystallized in rich to poor H_2O magma and in moderately oxidized to moderately reduced calc-alkaline to alkaline magmas (Erdmann *et al.* 2014). However, it was considered by Erdmann *et al.* (2014) that the following equation, proposed by Ridolfi *et al.* (2010), would be most suitable to calculate temperature:

$$\begin{aligned} &T\,(^\circ C) = -\,151.487Si^* + 2041;\ Si^* \\ &= Si + (Al^{IV} / 15) - (2Ti^{IV}) - (Al^{VI} / 2) - (Ti^{VI} / 1.8) \\ &+ (Fe^{3+} / 9) + (Fe^{2+} / 3.3) + (Mg / 26) + (Ca^B / 5) \\ &+ (Na^B / 1.3) - (Na^A / 15) + (K^A / 2.3) \end{aligned}$$

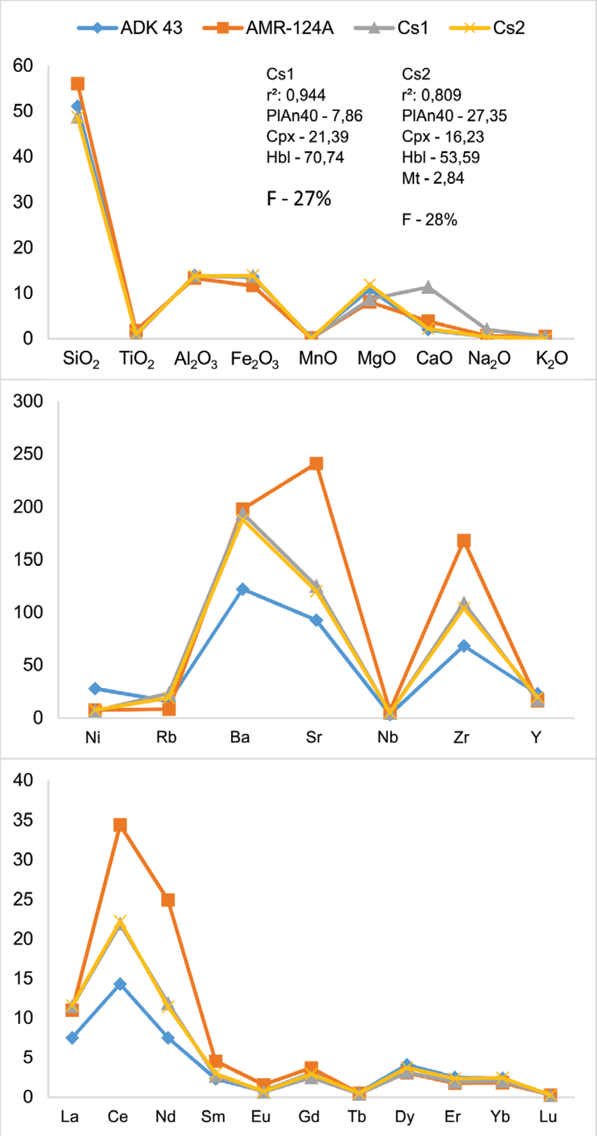

Figure 12. Partial melting modeling of the Horblend Gabbronorite (ADK-43, Marangoanha and Oliveira 2014) as a source of the Pedra Branca magma (AMR-124A, hornblende tonalite). (A) Major element modeling. (B) LILE and HFSE trace element modeling. (C) REE modeling.

The Ridolfi *et al.*'s (2010) geothermometer showed that the amphibole's temperature varies between 945 and 862°C. The dataset suggests an interval between 945 and 862°C for the liquidus temperature of the Pedra Branca magma (Tab. 2), which is consistent with the proposed mafic tholeiitic source proposed by Feio *et al.* (2013) and in this paper.

Pressure

The Al-in-hornblende geobarometer was proposed by Hammarstron and Zen (1986) and Hollister *et al.* (1987) to estimate the emplacement pressure of intermediate silicate plutons. The pressure calculation may match the granitoid emplacement. The Pedra Branca suite has an ideal paragenesis to use the geobarometers proposed by Hammarstron and Zen (1986) and Hollister *et al.* (1987), the plagioclase present in Pedra Branca suite (An < 25) are more sodic than the plagioclase founded in calc-alkaline granitoids in which the geobarometer was initially proposed (~An_{25-35}; Anderson and Smith 1995). Therefore, the geobarometers proposed by Hammarstron and Zen (1986), Hollister *et al.* (1987), Johnson and Rutherford (1989), and Schmidt (1992) was used to determine the pressure (Tab. 3).

The Hammarstron and Zen's (1986) geobarometer indicates pressure varying between 8–6 and 4.3 Kbar. The Schmidt's (1992) one indicates pressures between 8.6 and 4.8 Kbar. The pressures obtained, according to Hollister *et al.* (1987), was 9.3–4.4 Kbar. The model proposed by Johnson and Rutherford (1989) indicated values varying between 7.1 and 3.4 Kbar. The Fe/(Fe + Mg) *vs.* Al^{IV}+Al^{VI} diagram (Fig. 15A) indicated pressure between 7.4 and 4.5 Kbar.

According to the data obtained in this and in previous works (Feio *et al.* 2013), the Pedra Branca magma was derived from a lower tholeiitic mafic crust, so the pressure related to the magma source can be estimated between 9.3 and 7.1 Kbar, based on the proposed lower crustal source. On the order hand, these granitoids present intense deformation, magmatic banding, sub-vertical foliation, and local lineation caused by ductile deformation (Gomes and Dall'Agnol 2007), probably generated during the emplacement. These features indicate pluton emplacement in mesozone, possibly corresponding to the lower pressures of 4.8–3.4 Kbar. Thus, it is possible to conclude that pressures around 9.3–7.1 Kbar correspond to the magma source, and pressures around 3.4–4.8 Kbar represent the emplacement of the Pedra Branca suite (Tab. 3).

Oxygen fugacity

The PBS has a high to intermediate $FeO_t/(FeO_t + MgO)$ ratio (0.60–0.97) varying according to the lithology (Tab. 1). The tonalites have a 0.60–0.83 ratio, and the trondhjemites, 0.91–0.97. Amphibole shows low ratios around 0.51–0.59, similarly to the tonalite ratios, which indicate high oxygen fugacity according to the Fe/(Fe+Mg) *vs.* Al^{IV} diagram (Fig. 15B).

Petrographic data show ilmenite as the main opaque mineral in the Pedra Branca suite, occurring mainly in tonalites. The FeOt/(FeOt + MgO) ratio of this lithology and Fe/(Fe + Mg) ratio in amphibole indicate an equilibrium between rock crystallization and these mineral phases. On the order hand, magnetite was found only in one sample (AMR-191) with a 0.96 FeOt/(FeOt+MgO) ratio.

Thus, it can be affirmed that tonalites are classified as oxidized granitoids from the Magnetite series (Ishihara 1997), and trondhjemites are lightly oxidized to reduced.

Water content

The water content necessary to stabilize amphibole varies along with pressure: 2.0–4.0 Kbar requires 4% of water, 5% of the water in pressures around 4.0 Kbar, and 7–9% in a 9.6 Kbar pressure are necessary to stabilize amphibole without pyroxene in a silicate magma (Naney 1983, Dall'Agnol *et al.* 1999, Klimm *et al.* 2003, Prouteau and Scaillet 2003, Bogaerts *et al.* 2006). Clinopyroxene relicts occur in the Pedra Branca suite (Gomes and Dall'Agnol 2007) and are scarce and located, which suggests that clinopyroxene was stable during initial magma state and almost totally reacted during cooling (Naney 1983, Dall'Agnol *et al.* 1999).

Thus, it is possible to affirm that these tonalites and trondhjemites are derived from magmas with more than 4% H_2O, and depending on the assumed pressure crystallization, possibly around or even more than 7%. This evidence is endorsed by the absence of clinopyroxene crystals.

Petrogenesis

The tonalites from PBS were originated from the partial melting of rocks with compositional similarities with diabase from Nova Canadá (Marangoanha and Oliveira 2014). According to Marangoanha and Oliveira (2014), these diabases are post-Archean, so they are not the real source of PBS. However, we consider that the real source of PBS had similar features if compared to the Nova Canadá diabase. These data match with the geochemical modeling, which shows that the tonalites were derived from a partial melting with a residue containing hornblende, plagioclase, and clinopyroxene, and may or may not have magnetite. It is worth pointing out that according to Marangoanha and Oliveira (2014), the diabase from Nova Canadá is enriched in Y (14.9 to 63.9 ppm) and Zr (56.1 to 236.6 ppm). The sample used in the modeling was a diabase classified as hornblende-grabbronorite (ADK 43, Marangoanha and Oliveira 2014), as representative of the magma source. Therefore, it is possible to affirm that the HFSE enrichment in the granitoids of the Pedra Branca suite is derived directly from the source and not associated with the order process as hydrothermal alteration.

For the trondhjemites, it is proposed that they were originated by the same processes (partial melting) as tonalites, from similar but not identical sources, probably with lower melting degrees than tonalites, and evolved as two different liquids throughout magmatic differentiation.

Geotectonic setting

A subduction setting does not seem capable of explaining the genesis of Pedra Branca magma (2.75 Ga; Feio *et al.* 2013, Sardinha *et al.* 2004), considering the opening and closing of the Carajás rift occurred during the Neoarchean (2.76–2.68 Ga; Tavares 2015, Gibbs *et al.* 1986), which was responsible for generating the metavolcanic rocks of the Itacaiunas Supergroup (2.76–2.73 Ga; Machado *et al.* 1991). Moreover, several A-type granites were formed in the Carajás Basin, and Canaã dos Carajás Domain during Neoarchean, such as the Estrela Granitic Complex (2.76 Ga, Barros *et al.* 2001), Serra do Rabo granite (2.74 Ga, Sardinha *et al.* 2006) and Planalto granite (2.74–2.73 Ga; Feio *et al.* 2013). This evidence indicates that, during the Neoarchean, there was a continental intraplate setting in the CB and the CCD. Also, the hypothesis of an extensional continental setting for this region is ratified by the presence of Diopside-Norite Pium, which was dated from 3.0 Ga and metamorphosed in 2.85 Ga (Pidgeon *et al.* 2000). However, recent research shows that this unit in the Canãa area was crystallized 2.74 Ga (Santos *et al.* 2013a) in an extensional setting.

The accentuated crustal thickening associated with the formation of Itacaiunas shear belt, the elevated geothermal gradient in the Archean and the high volume of magma generation during the Neoarchean in the Canaã dos Carajás Domain and Carajás basin indicate that there was an expressive thermal anomaly in the Canaã dos Carajás area (Gomes and Dall'Agnol 2007). The small

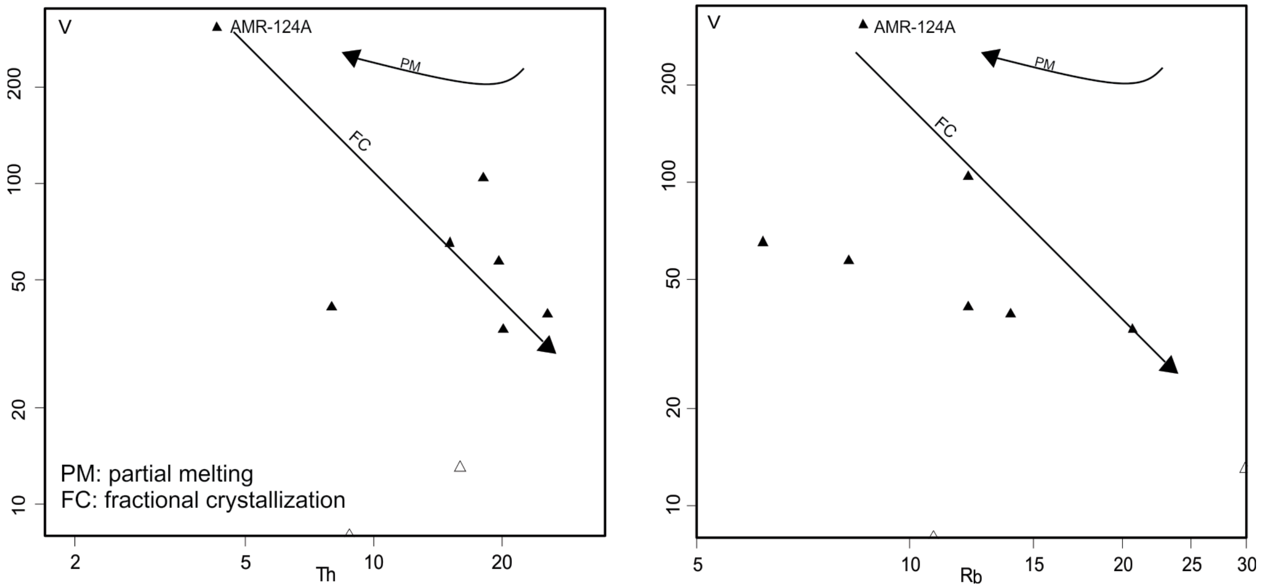

Figure 13. Log diagrams of compatible elements (V) *vs*. Incompatible elements (Th and Rb). Symbology according to Figure 3.

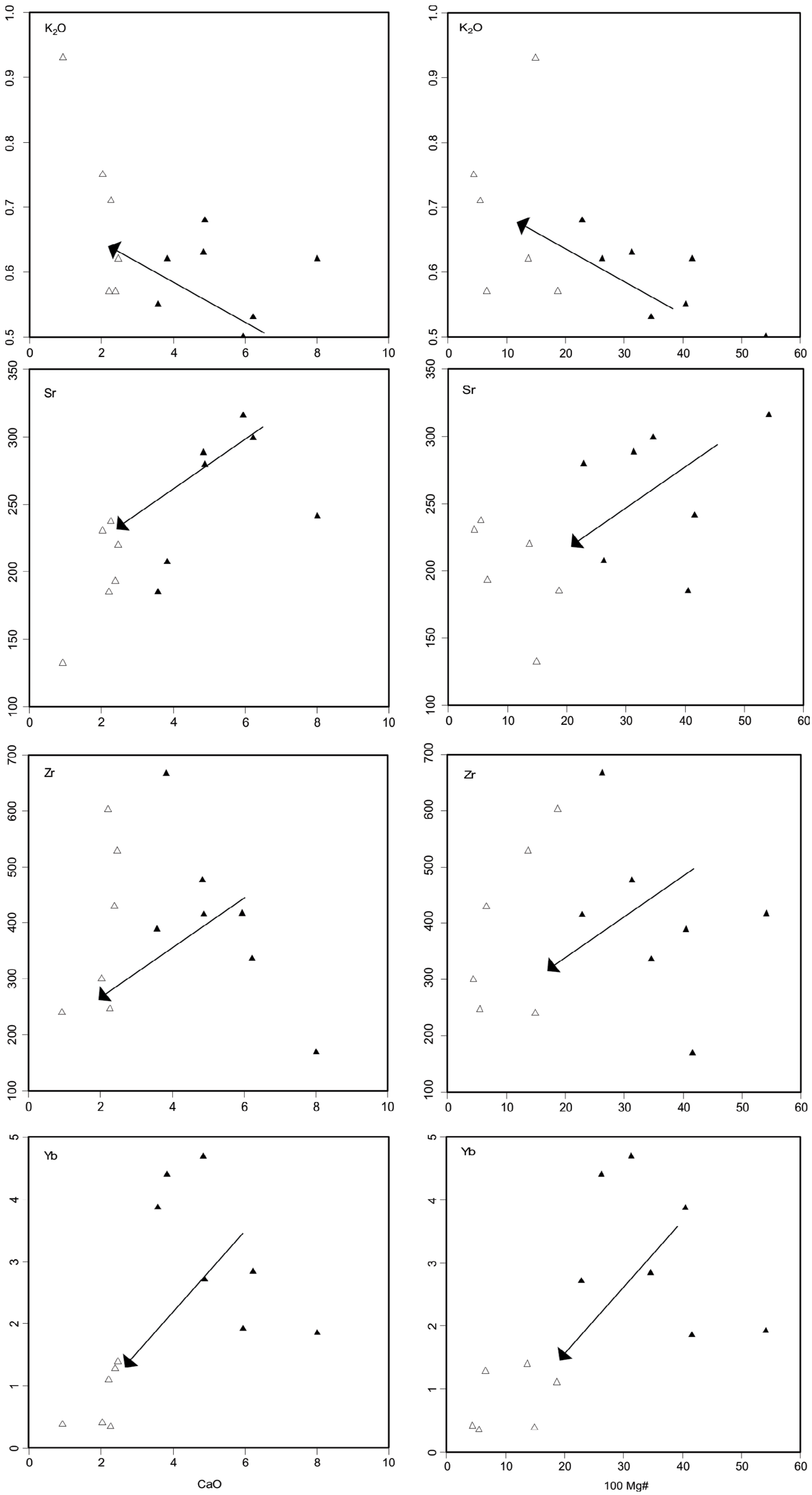

Figure 14. Covariance diagrams between the wt% CaO (a) and 100×Mg# (b) against the wt% K_2O, Sr, Zr, and Yb (ppm) for the rocks of the Pedra Branca suite. Arrow indicates vectors to the residual liquids of the suite. Symbology according to Fig. 3.

volume of Pedra Branca bodies associates its genesis to lower continental crust partial melting (continental tholeiitic gabbros composition) generated in an extensional setting (Carajás Rifte) just like Diopside-Norite Pium (Santos *et al.* 2013a). This granitic magmatism and associated Neoarchean mafic volcanism related to Grão-Pará group (Martins *et al.* 2017), and other mafic bodies in Canaã and adjacent areas (Lafon *et al.* 2000, Machado *et al.* 1991) might have been responsible for such high temperatures (almost 1,000°C) in a rift setting.

Zhang *et al.* (2012) studied the generation of TTG magmas associated with partial melting from the lower continental crust, in the North China Craton. According to these authors, the Neoarchean trondhjemites with high- and low-Al are contemporaneous and were formed by partial melting of the juvenile lower crust induced by magma underplating to form the high-Al group and the intraplate to low-Al.

Why the Pedra Branca Suite Diverge From Typical Archean TTGs?

The unique geochemical features can be explained by three reasons:

- The magmatic source has different geochemical and mineralogical features than typical TTG, which are related to partial melting of garnet-amphibolite or eclogite under varying conditions of fluids presence (Martin 1994, Martin and Moyen 2002, Moyen *et al.* 2003); on the order hand, PBS rocks are associated with the partial melting of continental tholeiitic grabbros;
- The PBS was originated in a distinct geotectonic setting. TTG are associated with the partial melting of basalts from a thickened oceanic crust (Smithies 2000, Condie 2005) or to subduction of a basaltic oceanic crust (Condie 1989, Martin 1994, Rollison 1993, Martin and Moyen 2002, Moyen *et al.* 2003); on the order hand, PBS were originated from partial melting of continental gabbros in an extensional setting (Carajás Rift);
- The high water content in Pedra Branca magma (up to 4%) diverge from TTG's magmas. According to Moyen and Stevens (2006), based on experimental petrology studies, the partial melting that originate TTG's magma can be divided according to the fluids content. These authors emphasize mainly the fluid-absent melting; the water content in this process

Table 3. Estimate of pressure and temperature of crystallization for the tonalites and trondhjemites of the Pedra Branca suite.

Pedra Branca suite	**Tonalite**	
Samples	**AMR – 121A**	**AMR – 124A**
Pressure (kbar)		
Al total	1.89 – 2.16	1.63 – 2.50
Hammarstron and Zen (1986)	5.4 – 6.9	4.3 – 8.6
Schmidt (1992)	5.8 – 7.2	4.9 – 8.9
Hollister *et al.* (1987)	5.7 – 7.4	4.4 – 9.3
Johnson and Rutherford (1989)	4.4 – 5.7	3.4 – 7.1
Anderson and Smith (1995)	5.8 – 7.3	4.5 – 6.1
Temperature (°C)		
Ridolfi *et al.* (2010)	888 – 905	862 – 945

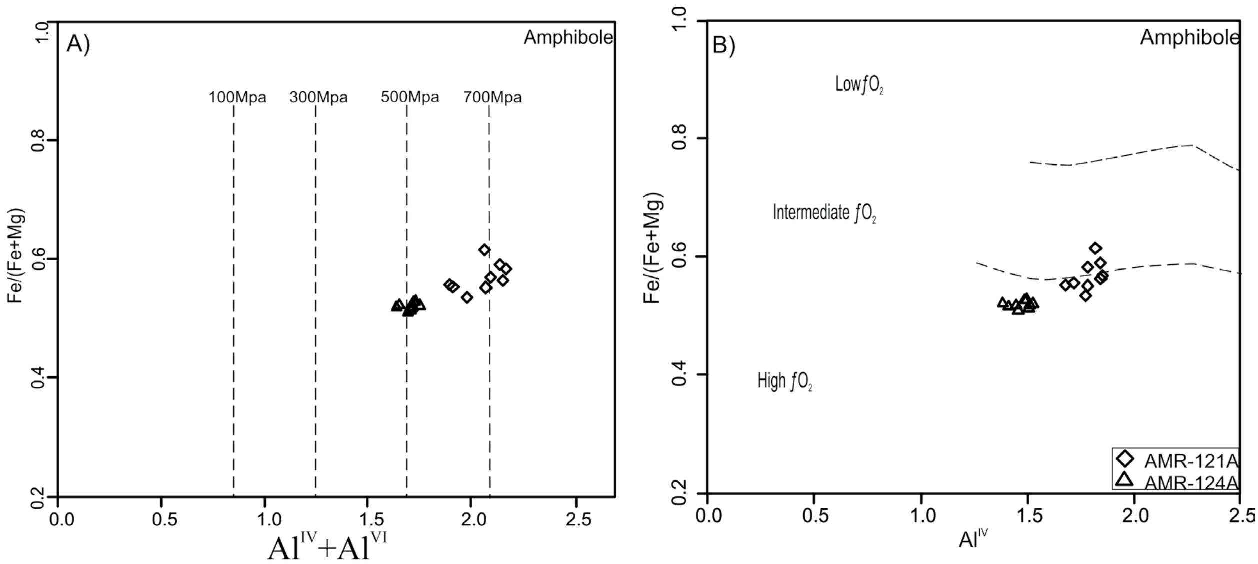

Figure 15. (A) Fe/(Fe+Mg) *vs.* Al^{IV} + Al^{VI} diagram showing the compositional variation of amphibole of the Pedra Branca Suite. Crystallization pressure ranges according to Anderson and Smith (1995); (B) Fe/(Fe+Mg) *vs.* Al^{IV} diagram showing the compositional variation of amphibole of the Pedra Branca Suite. Low, Intermediate and High *f*O2 fields according to Anderson and Smith (1995).

comes only from hornblende breakdown, which can generate less than 1.8 wt% H_2O in these magmas.

Comparison with other Neoarchean TTGs and similar rocks

The Pedra Branca suite has unique features that differ from the Archean TTG. For this reason, similar rocks like PBS have not been previously described in the literature. Gomes and Dall'Agnol (2007) compared the suite to Paleoarchean grey gneisses (3,42 Ga) from Sete Voltas Massif, São Francisco Craton. According to Martin (1997), these rocks show positive anomalies of Zr (142-288 ppm) and Nb (6-13 ppm), similar to PBS.

In the Mineiro Belt, Seixas *et al.* (2012) described the Lagoa Dourada Suite (2.3 Ga) a TTG suite enriched in Zr (140–261 ppm), Nb (4.5–8.2 ppm), and relatively in Y (5–11 ppm). Also in the Mineiro Belt, tonalites from the Alto Maranhão Suite also have high contents of Zr (150 to 238 ppm), Y (11 to 20 ppm), and low Rb content (40–94 ppm) (Seixas *et al.* 2013).

In the Amazonian Craton, Vila União tonalites, central portion of Canaã dos Carajás Domain, are similar to PBS. The main ferromagnesian minerals are hornblende and biotite, are relatively enriched in TiO_2 (0.76 to 1.51 wt%) and have a high content of HFSE Zr (529.00–936.80 ppm), Y (34.80–56.00 ppm), and Nb (14.50–18.90) (Oliveira *et al.* 2018).

CONCLUSIONS

- Tonalites are metaluminous, and trondhjemites vary from peraluminous and metaluminous. They both belong to the subalkaline low-K series, which are calc and ferroan granitoids;
- The magmatic differentiation process among the suite members was possibly controlled by crystal accumulation during the magmatic flow;
- Amphibole is classified as ferroan edenite and hastingsite. Plagioclase is oligoclase. Titanite is a primary igneous mineral that was reequilibrated during a deformational or metamorphic event;
- A temperature interval of 862–945°C was concluded for the initial crystallization of the Pedra Branca suite. Pressures of 9.3–7.1 kbar for the origin and 4.8–3.4 kbar for the emplacement of the Pedra Branca magma. The dominance of amphibole and biotite among the mafic minerals of the Planalto Suite and the typical absence of pyroxene indicate that the water content in the magma was higher than 4 wt% and could even exceed 7 wt%;
- Pedra Branca Magma originated from the partial melting of continental tholeiitic gabbros, in an extensional setting (Carajás Ritfte). This process left a residue containing plagioclase, hornblende, clinopyroxene and may or may not have magnetite. The magma source had chemical-mineralogical features similar to Nova Canadá Diabase (Marangoanha and Oliveira 2014) and not rocks similar to Serra Geral Basalts, as affirmed by Gomes and Dall'Agnol (2007); another divergence is about the fusion degree, those authors affirmed that the Pedra Branca bodies were formed by a low scale fusion, however, according to the geochemical modeling, fusion degree was ~28%;
- The enrichment in HFSE in these granitoids is derived directly from the source rock and is not related to the order process as hydrothermal alteration;
- Pedra Branca suite diverges from typical Archean TTG, due to the derivation from a different source, formed in a different geotectonic setting proposed to most TTG, and by the presence of elevated quantities of water in the magma if compared to typical TTG;
- In geochemical and petrographic terms, it is similar to Vila União tonalites (Oliveira *et al.* 2018), both units have high HFSE content and hornblende and biotite as ferromagnesian minerals.

ACKNOWLEDGMENTS

The Grupo de Petrologia de Granitoides from Universidade Federal do Pará are acknowledged for their support in geological mapping and previous works in the studied area. M.J James is acknowledged for her support in writing, and P.V.F.S Alves for helping with the EPMA analysis. The reviews by Silvio RF Vlach, an anonymous reviewer, and the editorial handling of C. Ricominni were greatly appreciated and helped to improve the original manuscript. This research received financial support from CNPq (R. Dall'Agnol — Grants 0550739/2001-7, 476075/2003-3, 307469/2003-4, 484524/2007-0; PRONEX — Proc. 66.2103/1998-0; G.R.L Feio — CNPq scholarship), and Universidade do Sul e Sudeste do Pará (Unifesspa).

ARTICLE INFORMATION

Manuscript ID: 20190093. Received on: 09/14/2019. Approved on: 06/05/2020.
A.S.S. participated in the whole study and wrote most part of the manuscript, including the construction of the figures and tables. Also, he corrected the manuscript according to the reviewer's suggestions. G.R.L.F. conceptualized the original idea and improved and reviewed the original draft. J.P.S.A. was responsible for writing the original parts of mineral chemistry and crystallization parameters. R.D. was responsible for the conceptualization and review of the original draft and helped review the magmatic differentiation. J.A.C.A. reviewed the original draft. A.C.B.G. obtained original geochemical data and helped in the petrogenetic setting.
Competing interests: The authors declare no competing interests.

REFERENCES

Aleinikoff N.J., Wintsch R.P., Fanning C.M., Dorais M.J. 2002. U-Pb geochronology of zircon and polygenetic titanite from the Glastonbury Complex, Connecticut,USA: an integrated SEM, EMPA, TIMS, and SHRIMP study. *Chemical Geology*, **188**(1-2):125-147. http://doi.org/10.1016/S0009-2541(02)00076-1

Almeida J.A.C., Dall'agnol R., Rocha M.C. 2017. Tonalite–trondhjemite and leucogranodiorite–granite suites from the Rio Maria domain, Carajas Province, Brazil: implications for discrimination and origin of the Archean Na-granitoids. *The Canadian Mineralogist*, **55**(3):437-456. http://doi.org/10.3749/canmin.1600068

Almeida J.A.C., Dall'Agnol R., Oliveira M.A., Macambira M.J.B., Pimentel M.M., Rämö O.T., Guimarães F.V., Leite A.A.S. 2011. Zircon geochronology, geochemistry and origin of the TTG suites of the Rio Maria granite-greenstone terrane: Implications for the growth of the Archean crust of the Carajás province, Brazil. *Precambrian Research*, **187**(1-2):201-221. http://doi.org/10.1016/j.precamres.2011.03.004

Althoff F.J., Barbey P., Boullier A.M. 2000. 2.83. Ga plutonism and deformation in the SE Amazonian craton: the Archean granitoids of Marajoara (Carajas Mineral Province, Brazil). *Precambrian Research*, **104**(3-4):187-206. https://doi.org/10.1016/S0301-9268(00)00103-0

Anderson J.L., Smith D.R 1995. The effects of temperature and ƒO2 on the Al-in-hornblende barometer. *American Mineralogist*, **80**:549-559.

Arth J.G., Barker F., Peterman Z.E., Friedman I. 1978. Geochemistry of the gabbro—diorite—tonalite—trondhjemite suite of southwest Finland and its implications for the origin of tonalitic and trondhjemitic magmas. *Journal of Petrology*, **19**(2):289-316. https://doi.org/10.1093/petrology/19.2.289

Barker F. 1979. Trondhjemite: definition, environment and hypotheses of origin. *Developments in Petrology*, **6**:1-12. https://doi.org/10.1016/B978-0-444-41765-7.50006-X

Barker F., Arth J.G. 1976. Generation of trondhjemitic-tonalitic liquids and Archean bimodal trondhjemite-basalt suites. *Geology*, **4**(10):596-600. https://doi.org/10.1130/0091-7613(1976)4<596:GOTLAA>2.0.CO;2

Barros C.E.M., Macambira M.J.B., Barbey P. 2001. Idade de zircões do Complexo Granítico Estrela: relações entre magmatismo, deformação e metamorfismo na Província Metalogenética de Carajás. *In*: Simpósio de Geologia da Amônia, 7., 2001. *Proceedings*... p. 17-20.

Bogaerts M., Scaillet B., Auwera J.V. 2006. Phase equilibria of the Lyngdal granodiorite (Norway): implications for the origin of metaluminous ferroan granitoids. *Journal of Petrology*, **47**(12):2405-2431. https://doi.org/10.1093/petrology/egl049

Champion D.C., Smithies R.H. 2003. Archaean granites. *In*: Magmas to Mineralisation: The Ishihara Symposium, 2003, Australia. *Geoscience*… p. 19-24.

Cocherie A. 1986. Systematic Use of Trace Element Distribution on Patterns in Log-Log Diagrams. *Geochimica et Cosmoshimica Acta*, **50**(11):2517-2522. https://doi.org/10.1016/0016-7037(86)90034-7

Condie K.C. 1989. Geochemical changes in basalts and andesites across the Archean-Proterozoic boundary: Identification and significance. *Lithos*, **23**(1-2):1-18. https://doi.org/10.1016/0024-4937(89)90020-0

Condie K.C. 1993. Chemical composition and evolution of the upper continental crust: contrasting results from surface samples and shales. *Chemical Geology*, **104**(1-4):1-37. https://doi.org/10.1016/0009-2541(93)90140-E

Condie K.C. (Ed.). 1994. *Archean crustal evolution*. United States: Elsevier Science, 543 p.

Condie K.C. 2005. TTGs and adakites: are they both slab melts? *Lithos*, **80**(1-4):33-44. https://doi.org/10.1016/j.lithos.2003.11.001

Dall'Agnoll R., Oliveira D.C., Guimarães F.V., Gabriel E.O., Feio G.R.L., Lamarão C.N., Rodrigues D.S. 2013. Geologia do subdomínio de transição do Domínio Carajás–Implicações para a evolução arqueana da Província Carajás–Pará. *In:* Simpósio de Geologia da Amazônia, 13., Belém. *Proceedings*...

Dall'Agnol R., Oliveira M.A., Almeida J.A.C., Althoff F.J., Leite A.A.S., Oliveira D.C., Barros C.E.M. 2006. Archean and paleoproterozoic granitoids of the CarajasMetallogenetic province, eastern Amazonian craton. *In*: Dall'Agnol R., Rosa-Costa L.T., Klein E.L. (Eds.), *Symposium on Magmatism, Crustal Evolution, and Metallogenesis of the Amazonian Craton*. Abstracts Volume and Field Trips Guide. Belém, PRONEX-UFPA/SBG-NO, p. 99-150.

Dall'agnol R., Scaillet B., Pichavant M. 1999. An experimental study of a lower Proterozoic A-type granite from the eastern Amazonian Craton, Brazil. *Journal of Petrology*, **40**(11):1673-1698. https://doi.org/10.1093/petroj/40.11.1673

Erdmann S., Martel C., Pichavant M., Kushnir A. 2014. Amphibole as an archivist of magmatic crystallization conditions: problems, potential, and implications for inferring magma storage prior to the paroxysmal 2010 eruption of Mount Merapi, Indonesia. *Contributions to Mineralogy and Petrology*, **167**:1-23. https://doi.org/10.1007/s00410-014-1016-4

Feio G.R.L., Dall'Agnol R., Dantas E.L., Macambira M.J.B., Gomes A.C.B., Sardinha A.S., Oliveira D.C., Santos R.D., Santos P.A. 2012. Geochemistry, geochronology, and origin of the Neoarchean Planalto Granite suite, Carajás, Amazonian craton: A-type or hydrated charnockitic granites?. *Lithos*, **151**:57-73. https://doi.org/10.1016/j.lithos.2012.02.020

Feio G.R.L., Dall'Agnol R., Dantas E.L., Macambira M.J.B., Santos J.O.S., Althoff F.J., Soares J.E.B. 2013. Archean granitoid magmatism in the Canaã dos Carajás area: implications for crustal evolution of the Carajás province, Amazonian craton, Brazil. *Precambrian Research*, **227**:157-185. https://doi.org/10.1016/j.precamres.2012.04.007

Frost B.R., Barnes C.G., Collins W.J., Arculus R.J., Ellis D.J., Frost C.D. 2001. A geochemical classification for granitic rocks. *Journal of Petrology*, **42**(11):2033-2048. https://doi.org/10.1093/petrology/42.11.2033

Gabriel E.O., Oliveira D.C. 2014. Geologia, petrografia e geoquímica dos granitoides arqueanos de alto magnesio da região de Agua Azul do Norte, porção sul do Domínio Carajás, Pará. *Boletim do Museu Paraense Emílio Goeldi Ciências Naturais*, **9**(3):533-564.

Gibbs A.K., Wirth K.R., Hirata W.K., Olszewski Jr. W.J. 1986. Age and composition of the Grão Pará Group volcanics, Serra dos Carajás, Brazil. *Revista Brasileira de Geociências*, **16**(2):201-211.

Gomes A.C.B. 2003. *Geologia, petrografia e geoquímica dos granitóides de Canaã dos Carajás, SE do Estado do Pará. Belém*. MS Dissertation, Centro de Geociências, Universidade Federal do Pará, Belém, 261 p.

Gomes A.C.B., Dall'agnol R. 2007. Nova associação tonalítica-trondhjemítica neoarqueana na região de Canaã dos Carajás: TTGS com altos conteúdos de Ti, Zr e Y. *Revista Brasileira de Geociências*, **37**(1):182-193. http://doi.org/10.25249/0375-7536.2007371182193

Guimarães F.V., Dall'Agnol R., Almeida J.D.A.C., Oliveira M.A. 2010. Caracterização geológica, petrográfica e geoquímica do Trondhjemito Mogno e Tonalito Mariazinha, Terreno Granito-Greenstone mesoarqueano de Rio Maria, SE do Pará. *Revista Brasileira de Geociências*, **40**(2):196-211.

Hammarstron J.M., Zen E.A. 1986. Aluminum in hornblende: an empirical igneous geobarometer. *American Mineralogist*, **71**:1297-1313.

Hollister L.S., Grissom G.C., Peters E.K., Stowell H.H., Sisson V.B. 1987. Confirmation of the empirical correlation of Al in hornblende with pressure of solidification of calc-alkaline plutons. *American Mineralogist*, **72**(3-4):231-139.

Ishihara S. 1997. The magnetite-series and ilmenite-series granitic rocks. *Mining Geology*, **27**(145):293-305. https://doi.org/10.11456/shigenchishitsu1951.27.293

Janoušek V., Bowes D.R., Rogers G., Farrow C.M., Jelínek E. 2000. Modelling diverse processes in the petrogenesis of a composite batholith: the Central Bohemian Pluton, Central European Hercynides. *Journal of Petrology*, **41**(4):511-543. https://doi.org/10.1093/petrology/41.4.511

Johnson M.C., Rutherford M.J. 1989. Experimental calibration of the aluminium-in-hornblende geobarometer with application to Long Valley caldera (California) volcanic rocks. *Geology*, **17**(9):837-841. https://doi.org/10.1130/0091-7613(1989)017%3C0837:ECOTAI%3E2.3.CO;2

Kalsbeek F. 2001. Geochemical comparison between Archaean and Proterozoic orthogneisses from the Nagssugtoqidian orogen, West Greenland. *Precambrian Research*, **105**(2-4):165-181. https://doi.org/10.1016/S0301-9268(00)00110-8

Kepezhinskas P.K., Defant M.J., Drummond M.S. 1995. Na metasomatism in the island-arc mantle by slab melt—peridotite interaction: evidence from mantle xenoliths in the North Kamchatka Arc. *Journal of Petrology*, **36**(6):1505-1527. https://doi.org/10.1093/oxfordjournals.petrology.a037263

Klimm K., Holtz F., Johannes W., King P.L. 2003. Fractionation of metaluminous A-type granites: an experimental study of the Wangrah suite, Lachlan Fold Belt, Australia. *Precambrian Research*, **124**(2-4):327-341. https://doi.org/10.1016/S0301-9268(03)00092-5

Kowallis B.J. Christiansen E.H., Griffen D.T. 1997. Compositional variations in titanite. *Geological Society of America Abstracts with Programs*, **29**(6):402.

Lafon J. M., Macambira M.J.B., Pidgeon R.T. 2000. Zircon U-Pb SHRIMP dating of Neoarchean magmatism in the southwestern part of the Carajás Province (eastern Amazonian Craton, Brazil). *In*: International Geological Congress, 31., 2000. *Proceedings*…

Leake B.E., Wooley A.R., Arp C.E.S., Birch W.D., Gilbert M.C., Grice J.D., Hawthorne F.C., Kato A., Kisch H.J., Krivovichev V.G., Linthout K., Laird J., Mandarino J.A., Maresch W.V., Nickel E.H., Rock N.M.S., Schumacher J., Smith J.C., Stephenson N.C.N., Ungaretti L., Whittaker E.J.W., Youzhi G. 1997. Nomenclature of amphiboles: report of the subcommittee on amphiboles of the international mineralogical association commission on new minerals and Mineral names. *The Canadian Mineralogist*, **61**(405):295-321. https://doi.org/10.1180/minmag.1997.061.405.13

Le Maitre R.W. 2002. Igneous Rocks. A Classification and Glossary of Terms. Recommendations of the International Union of Geological Sciences Subcommission on the Systematics of Igneous Rocks. 2ª ed. Cambridge, New York, Melbourne, Cambridge University Press, 236 p.

Leite A.A.D.S., Dall'Agnol R., Macambira M.J.B., Althoff F.J. 2016. Geologia e geocronologia dos granitóides arqueanos da região de Xinguara-PA e suas implicações na evolução do terreno granito-greenstone de Rio Maria, Cráton Amazônico. *Revista Brasileira de Geociências*, **34**(4):447-458.

Macambira M.J.B., Lafon J.M. 1995. Geocronologia da Província Mineral de Carajas;Síntese dos dados e novos desafios. *Boletim do Museu Paraense Emílio Goeldi, Série Ciências da Terra*, **7**:263-287.

Machado N., Lindenmayer Z., Krogh T.E., Lindenmayer D. 1991. U/Pb geochronology of Archean magmatism and basement reactivation in the Carajás Área, Amazon shield, Brazil. *Precambrian Research*, **49**(3-4):329-354. https://doi.org/10.1016/0301-9268(91)90040-H

Marangoanha B., Oliveira D.C. 2014. Diabásios e anfibolitos da área de Nova Canadá: natureza e implicações tectônicas para a Província Carajás. *Boletim do Museus Paraense Emílio Goeldi Ciências Naturais*, **9**(3):565-596.

Martin H. 1986. Effect of steeper Archean geothermal gradient on geochemistry of subduction-zone magmas. *Geology*, **14**(9):753-756. https://doi.org/10.1130/0091-7613(1986)14<753:EOSAGG>2.0.CO;2

Martin H. 1987. Petrogenesis of Archean trondhjemites, tonalites and granodiorites from eastern Finland: major and trace element geochemistry. *Journal of Petrology*, **28**:921–953. https://doi.org/10.1093/petrology/28.5.921

Martin H. 1994. The Archean grey gneisses and the genesis of continental crust. *Developments in Precambrian Geology*, **11**:205-259. https://doi.org/10.1016/S0166-2635(08)70224-X

Martin H., Moyen J.-F. 2002. Secular changes in TTG composition as markers of the progressive cooling of the Earth. *Geology*, **30**(4):319-322. https://doi.org/10.1130/0091-7613(2002)030<0319:SCITTG>2.0.CO;2

Martin H., Peucat J.J., Sabaté J.C., Cunha J.C. 1997. Crustal evolution in the Archaean of South America: example of the Sete Voltas Massif, Bahia State, Brazil. *Precambrian Research*, **82**(1-2):35-62. https://doi.org/10.1016/S0301-9268(96)00054-X

Martin H., Smithies R.H., Rapp R., Moyen J.-F., Champion D. 2005. An overview of adakite, tonalite–trondhjemite–granodiorite (TTG), and sanukitoid: relationships and some implications for crustal evolution. *Lithos*, **79**(1-2):1-24. https://doi.org/10.1016/j.lithos.2004.04.048

Martins P.L.G., Toledo C.L.B., Silva A.M., Chemale Jr. F., Santos J.O.S., Assis L.M. 2017. Neoarchean magmatism in the southeastern Amazonian Craton, Brazil: Petrography, geochemistry and tectonic significance of basalts from the Carajás Basin. *Precambrian Research*, **302**:340-357. https://doi.org/10.1016/j.precamres.2017.10.013

Moreto C.P.N., Monteiro L.V.S. Xavier R.P., Amaral W.S., Santos T.J.S., Juliani C., Souza Filho C.R. 2011. Mesoarchean (3.0 and 2.86 Ga) host rocks of the iron oxide–Cu–Au Bacaba deposit, Carajás Mineral Province: U–Pb geochronology and metallogenetic implications. *Mineralium Deposita*, **46**(7):789-811. https://doi.org/10.1007/s00126-011-0352-9

Moyen J-F. 2011. The composite Archaean grey gneisses: Petrological significance, and evidence for a non-unique tectonic setting for Archaean crustal growth. *Lithos*, **123**(1-4): 21-36. https://doi.org/10.1016/j.lithos.2010.09.015

Moyen J.F., Martin H. 2012. Forty years of TTG research. *Lithos*, **148**:312-336. https://doi.org/10.1016/j.lithos.2012.06.010

Moyen J.F., Martin H., Jayananda M., Auvray B. 2003. Late Archaean granites: a typology based on the Dharwar Craton (India). *Precambrian Research*, **127**(1-3):103-123. https://doi.org/10.1016/S0301-9268(03)00183-9

Moyen J.-F., Stevens G. 2006. Experimental constraints on TTG petrogenesis: implications for Archean geodynamics. *In*: Benn K., Mareschal J.-C., Condie K.C. (Eds.), *Archean geodynamics and environments*. Monographs AGU, p. 149-178.

Nakamura N. 1974. Determination of REE, Ba, Fe, Mg, Na and K in carbonaceous and ordinary chondrites. *Geochimica et Cosmochimica Acta*, **38**(5):757-775. https://doi.org/10.1016/0016-7037(74)90149-5

O'Connor J.T. 1965. A classification for quartz-rich igneous rocks based on feldspar ratios. *US Geological Survey Professional Paper B*, **525**:79-84.

Oliveira M.A., Dall'Agnol R., Scaillet B. 2010a. Petrological constraints on crystallization conditions of Mesoarchean Sanukitoid Rocks, southeastern Amazonian Craton, Brazil. *Journal of. Petrology*, **51**(10):2121-2148. https://doi.org/10.1093/petrology/egq051

Oliveira D.C., Santos P.J.L., Gabriel E.O., Rodrigues D.S., Faresin A.C., Silva M.L.T., Sousa S.D., Santos R.V., Silva A.C., Souza M.C., Santos R.D., Macambira M.J.B. 2010b. Aspectos geológicos e geocronológicos das rochas magmáticas e metamórficas da região entre os municípios de Agua Azul do Norte e Canaã dos Carajás e Província Mineral de Carajas. *In*: Congresso Brasileiro de Geoogia, 45., 2010, Belem. *Proceedings*... CD-ROM.

Oliveira V.E.S., Oliveira D.C., Marangoanha B., Lamarão C.N. 2018. Geology, mineralogy and petrological affinities of the Neoarchean granitoids from the central portion of the Canaã dos Carajás domain, Amazonian craton, Brazil. *Journal of South American Earth Sciences*, **85**:135-159. https://doi.org/10.1016/j.jsames.2018.04.022

Pidgeon R.T., Macambira M.J.B., Lafon J.M 2000. Th–U–Pb isotopic systems and internal structures of complex zircons from an enderbite from the Pium Complex, Carajás Province, Brazil: evidence for the ages of granulite facies metamorphism and the protolith of the enderbite.*Chemical Geology*, **166**(1-2):159-171. https://doi.org/10.1016/S0009-2541(99)00190-4

Prouteau G., Scaillet B. 2003 Experimental constraints on the origin of the 1991 Pinatubo dacite. *Journal of. Petrology*, **44**(12):2203-2241. https://doi.org/10.1093/petrology/egg075

Ridolfi F., Renzulli A. 2012. Calcic amphiboles in calc-alkaline and alkaline magmas: thermobarometric and chemometric empirical equations valid up to 1,130°C and 2.2 GPa. *Contributions Mineralogy Petrology*, **163**:877-895. https://doi.org/10.1007/s00410-011-0704-6

Ridolfi F., Renzulli A., Puerini M. 2010. Stability and chemical equilibrium of amphibole in calc-alkaline magmas: an overview, new thermobarometric formulations and application to subduction-related volcanoes. *Contributions to Mineralogy and Petrology*, **160**(1):45-66. https://doi.org/10.1007/s00410-009-0465-7

Rodrigues D.S., Oliveira D.C., Macambira M.J.B. 2014. Geologia, geoquímica e geocronologia do Granito Mesoarqueano Boa Sorte, município de Água Azul do Norte, Para e Província Carajas. *Boletim do Museu Paraense Emílio Goeldi Série Ciências Naturais*, **9**:597-633.

Rollison H. 1993. *Using geochemical data*. Evaluation, presentation, interpretation. Califórnia, Longman Scientific & Technical, 352 p.

Santos J.D., Hartmann L.A., Faria M.D., Riker S.R., Souza M.D., Almeida M.E., McNaughton N.J. 2006. A compartimentao do Crton Amazonas em provncias: avanços ocorridos no período 2000-2006. In: Simpósio de Geologia da Amazônia, 9, 2006. Proceedings... 2006.

Santos R.D., Galarza M.A., Oliveira D.C. 2013a. Geologia, geoquímica e geocronologia do Diopsídio-Norito Pium, Província Carajás. *Boletim do Museu Paraense Emílio Goeldi, Série Ciências da Terra*, **8**(3):355-382.

Santos J.D., Hartmann L.A., Faria M.D., Riker S.R., Souza M.D., Almeida M.E., McNaughton N.J. 2006. A compartimentação do Cráton Amazonas em províncias: avanços ocorridos no período 2000-2006. *In*: Simpósio de Geologia da Amazônia, 9., 2006. *Proceedings*...

Santos P.A., Teixeira M.F.B., Dall'Agnol R., Guimarães F.V. 2013b. Geologia, petrografia e geoquímica da associação Tonalito-Trondhjemito-Granodiorito (TTG) do extremo leste do subdomínio de transição, Província Carajas, Para. *Boletim do Museu Paraense Emílio Goeldi, Série Ciências Naturais*, **8**(3):257-290.

Santos P.J.L., Oliveira D.C. 2014. Trondhjemitos da área de Nova Canada: novas ocorrências de associações magmáticas tipo TTG no Domínio Carajás. *Boletim do Museu Paraense Emílio Goeldi Série Ciências Naturais*, **9**:635-659.

Sardinha A.S., Barros C.E.M., Krymsky R. 2006. Geology, geochemistry, and U–Pb geochronology of the Archean (2.74 Ga) Serra do Rabo granite stocks, Carajás Metallogenetic Province, northern Brazil. *Journal of South American Earth Sciences*, **20**(4):327-339.

Sardinha A.S., Dall'Agnol R., Gomes A.C.B., Macambira M.J.B., Galarza M.A. 2004. Geocronologia Pb–Pb e U–Pb em zircão de granitóides arqueanos da região de Canaã dos Carajás, Província Mineral de Carajás. *In*: Congresso Brasileiro de Geologia, 42., 2004, Araxá. *Proceedings*...

Schmidt M.W. 1992. Amphibole composition in tonalite as a function of pressure: An experimental calibration of the Al-in-hornblende barometer. *Contributions to Mineralogy and Petrology*, **110**:304-310. https://doi.org/10.1007/BF00310745

Seixas L.A.R., Bardintzeff J.M., Stevenson R., Bonin B. 2013. Petrology of the high-Mg tonalites and dioritic enclaves of the ca. 2130 Ma Alto Maranhão suite: Evidence for a major juvenile crustal addition event during the Rhyacian orogenesis, Mineiro Belt, southeast Brazil. *Precambrian Research*, **238**:18-41. https://doi.org/10.1016/j.precamres.2013.09.015

Seixas L.A.R., David J., Stevenson R. 2012. Geochemistry, Nd isotopes and U–Pb geochronology of a 2350 Ma TTG suite, Minas Gerais, Brazil: implications for the crustal evolution of the southern São Francisco craton. *Precambrian Research*, **196-197**:61-80. https://doi.org/10.1016/j.precamres.2011.11.002

Shand S.J. 1943. *Eruptive rocks:* their genesis, composition, classification, and their relation to ore deposits with a chaper on meteorites. New York, Hafner Pub. Co., 488 p.

Silva A.C., Dall'Agnol R., Guimarães F.V., Oliveira D.C. 2014. Geologia, petrografia e geoquímica de Associações Tonalíticas e Trondhjemíticas Arqueanas de Vila Jussara, Província Carajás, Pará. *Boletim do Museu Paraense Emílio Goeldi, Série Ciências Naturais*, **9**(1):13-45.

Smithies R.H. 2000. The Archaean tonalite–trondhjemite–granodiorite (TTG) series is not an analogue of Cenozoic adakite. *Precambrian Research*, **182**(1):115-125. https://doi.org/10.1016/S0012-821X(00)00236-3

Sousa F.S. 2015. *Caracterização morfológica e tipológica dos zircões do diopsídio Norito Pium, gnaisse Bom Jesus, suítes Pedra Branca e Planalto, Subdomínio de Transição, Província Carajás.* Course Conclusion Paper, Instituto de Geociências e Engenharias, Universidade Federal do Sul e Sudeste do Pará, Marabá, 61 p.

Souza Z.S., Potrel A., Lafon J.M., Althoff F.J., Pimentel M.M., Dall'Agnol R., Oliveira C.G. 2001. Nd, Pb and Sr isotopes in the Identidade belt, an Archaean greenstone belt of the Rio Maria region (Carajás Province, Brazil): implications for the Archaean geodynamic evolution of the Amazonian Craton. *Precambrian Research*, **109**(3-4):293-315. https://doi.org/10.1016/S0301-9268(01)00164-4

Takahashi E. 1986. Genesis of calc-alkali andesite magma in a hydrous mantle-crust boundary: Petrology of lherzolite xenoliths from the Ichinomegata crater, Oga peninsula, northeast Japan, part II. *Journal of Volcanology and Geothermal Research*, **29**(1-4):355-395. https://doi.org/10.1016/0377-0273(86)90051-X

Tassinari C.C.G., Macambira M.J.B. 2004. A evolução tectônica do Cráton Amazônico. *In*: Mantesso-Neto V., Bartorelli A., Carneiro C.D.R., Brito-Neves B.B. (Ed.), *Geologia do continente sul-americano:* evolução da obra de Fernando Flávio Marques de Almeida. São Paulo, Beca, p. 471-485.

Tavares F.M. 2015. *Evolução geotectônica do nordeste da Província Carajás*. PhD Thesis, Universidade Federal do Rio de Janeiro, Rio de Janeiro, 143 p.

Teixeira L.R. 2005. *GENESIS 4.0*—Software de Modelamento Geoquímico.

Teixeira M.F.B. 2017. *Estudos isotópicos de U-Pb, Lu–Hf e δ18o em zircão: implicações para a petrogênese dos granitos tipo-A paleoproterozóicos da província Carajás – Cráton Amazônico*. PhD Thesis, Universidade Federal do Pará, Belém, 218 p.

Tulloch A. 1979. Secondary Ca-Al silicates as low-grade alteration products of granitoid biotite. *Contributions to Mineralogy and Petrology*, **69**:105-117. https://doi.org/10.1007/BF00371854

Whitney D.L., Evans B.W. 2010. Symbols for rock-forming minerals. *American Mineralogist*, **95**(1):185-187. https://doi.org/10.2138/am.2010.3371

Wilson M. 1989. *Igneous petrogenesis:* a global tectonic approach. London, Unwin Hymann, 480 p.

Windley B.F. 1996. The evolving continents. New York: John Wiley & Sons. 785 p.

Zhang H., Zhai M.G., Santosh M., Li S.R. 2012. Low-Al and high-Al trondhjemites in the Huai'an Complex, North China Craton: Geochemistry, zircon U–Pb and Hf isotopes, and implications for Neoarchean crustal growth and remelting. *Journal of Asian Earth Sciences*, **49**:203-213. https://doi.org/10.1016/j.jseaes.2011.11.004